Subsurface Hydrothermal Activity Accompanying the 1990-1995 Eruption of Unzen Volcano Inferred from Self-Potential Observations(Dissertation_全文)

AUTHOR(S):

Hashimoto, Takeshi

主論文

Subsurface Hydrothermal Activity Accompanying the 1990-1995 Eruption of Unzen Volcano Inferred from Self-Potential Observations

by

Takeshi HASHIMOTO

Dissertation for the Degree of Doctor of Science

Department of Earth and Planetary Sciences,

Graduates School of Science, Kyoto University

January 1996

Acknowledgments

The author would like to express his grateful thanks to Dr. Yoshikazu Tanaka of Kyoto University for his guidance and supports on the whole of the author's study including this thesis. He sincerely understood the author's interests on the self-potential research in volcanic areas, and continuously encouraged him. This thesis could not have been completed without his hearty suggestions and careful reading of the manuscript.

The author would sincerely like to acknowledge to Professor Tohru Araki of Kyoto University, who gave him an opportunity to start this research. His guidance and stimulating comments encouraged the author.

The author wishes to express his special thanks to Professor Yoshimasa Kobayashi and Professor Norihiko Sumitomo of Kyoto University. Their instructive guidance and careful reading of the manuscript greately improved this thesis.

The author is deeply grateful to Professor Kazuya Ohta of Shimabara Earthquake and Volcano Observatory (SEVO), Kyushu University for his supporting the author's research. The author's observations in Unzen Volcano, which provided the fundamental data for this thesis, could not have been completed without his support.

The author expresses sincere thanks to Dr. Tsuneo Ishido of Geological Survey of Japan for fundamental and illuminating comments to the author's work. He kindly provided the author with the guidance of the studies of the electrokinetic phenomena.

The author deeply appreciates Dr. Naoto Oshiman of Kyoto University, Dr. Yasunori Nishida of Hokkaido University, and Dr. Yoichi Sasai of the Earthquake Research Institute (ERI), the University of Tokyo. They sincerely

understood his study and gave him helpful comments and hearty advice.

Special thanks are due to Dr. Tsuneomi Kagiyama, Dr. Hisashi Utada, and Mr. Fumio Masutani of ERI, the University of Tokyo for installing the observation system, cooperation in the field surveys, and also valuable discussions and suggestions.

The author wishes to express many thanks to Dr. Y. Sudo, Dr. S. Kikuchi, Dr. H. Ono, Dr. T. Tsutsui and other members of Aso Volcanological Laboratory (AVL), Kyoto University. The author could not have conducted his research without their wholehearted supports and encouragements. Mr. H. Masuda, Mr. M. Nakaboh, and Mr. Y. Matsumoto are greatly acknowledged for their collaboration of severe works in the field.

Special thanks are also extended to Dr. N. Matsuo, Dr. H. Shimizu, Dr. K. Umakoshi, and Dr. T. Matsushima of SEVO, Kyushu University for their unstinting supports to the author's research in Unzen Volcano. They kindly provided the author with great help in his performing the field observations in the volcano.

The author is deeply indebted to Dr. S. Machida of Kyoto University, Dr. T. Iyemori, Dr. T.Kamei, Dr. M. Takada of World Data Center C2 for geomagnetism, Kyoto University, for their continuous guidance and valuable comments. Mr. H. Kagami and other colleagues in the Geomagnetism and Space Magnetism research section of the Department of Earth and Planetary Sciences, Kyoto University are greatly acknowledged for valuable daily discussions and helpful comments in seminars.

Abstract

The evolution process of a hydrothermal system beneath the Unzen Volcano, one of the dacitic volcanoes in Shimabara peninsula, southwest Japan, was investigated by electric self-potential (SP) observations during the 1990-1995 eruption event. A distinct positive SP anomaly implying subsurface hydrothermal upwelling and its growth were detected by continuous observation in the vicinity of a lava dome which began extrusion in May, 1991. Besides, a negative SP anomaly, neighboring to the positive one, started to grow after the dome extrusion.

The SP changes accompanying the eruption can be mainly divided into three stages. We discuss the subsurface fluid flow corresponding to the SP change in each stage. Under the situation of shallow intrusion of magma, water discharge at the summit area seems to have resulted in the recharging movement of the surrounding ground water. The development of the negative SP with time is explained by growth of this shallow recharging flow. Such growth of the negative SP as well as the positive one provides a possible scheme of the establishment of a hydrothermal system or the cooling process of intruded magma close to the summit of the volcano.

Table of Contents

Section 1

General Introduction

1.1 A Brief Review of Self-Potential Studies

Origins of the electric potential in the earth are roughly divided into two groups. One is the induced potential by external magnetic or electric fields, while the other is the spontaneous potential caused by natural sources in the earth. The latter is called the Self-Potential (SP). The SP method, detection of subsurface conditions by SP on (normally) the ground surface, has been used for a long time in the field of mining for exploring undermined ore bodies. The oldest record of a SP observation is that conducted in 1830 (Sato and Mooney, 1960). Systematic surveys as one of the geophysical exploration methods seem to have started in 1920s. Recently the method has begun to be applied to geophysical investigations in volcanic or geothermal areas.

SP anomalies are often detected in active volcanic areas. In particular, positive SP anomalies, which are often correlated with fumarolic areas or thermal zones, are noted as a sign of subsurface hydrothermal upwelling. The idea associating SP anomalies with subsurface hydrothermal flow is based on the streaming potential theory. There is no promising candidate except the streaming potential for a mechanism which explains a positive SP anomaly greater than

several hundreds mV. Most of the recent SP studies have been performed in this scope. For example, Zablocki (1976) detected some positive SP anomalies corresponding to pit craters on Kilauea Volcano, Hawaii. It qualitatively explained the anomalies by shallow hydrothermal convection cells which have upwelling zones just under the pit craters. Similar positive SP anomalies are also detected on Usu, Me-akan, Hokkaido Komagatake (Nishida and Tomiya, 1987), Soufrier (Zlotnicki et al., 1994a), Piton de la Fournaise (Zlotnicki et al., 1994b) volcanoes. However these studies explained qualitatively the relationship between a positive SP anomaly and a subsurface hydrothermal upwelling, they have not reached to a quantitative relationship between SP and fluid flow. It was Ishido (1991) who combined quantitatively the equivalent electric current inferred from SP anomaly on the ground surface and the hydrothermal fluid flow under the ground. He estimated the intensity and the depth of an equivalent current source corresponding to the observed positive SP anomaly on Izu-Oshima Volcano and deduced subsurface hydrothermal fluid flow under the active crater using the equations of the electrokinetic phenomena in a porous medium.

Negative SP anomalies were often explained by the oxidation-reduction reaction of undermined mineral deposits in the age when the SP method was widely used for mineral explorations. However, recent investigators who are mainly interested in the relations between positive SP and hydrothermal upwelling have not paid much attention to negative SP anomalies. Few of the past studies referred to negative SP anomalies in volcanic or geothermal areas except Ishido et al. (1990) and Zohdy et al. (1973). The former mentioned that a negative SP

anomaly detected in Kirishima geothermal area could be attributed to the streaming potential due to local downward flow of the ground water and the latter correlated the positive and negative anomalies in Yellowstone geothermal area with subsurface upward and downward hydrothermal flow, respectively. Although their explanations are qualitative, it is important that these studies have pointed out the possibility of negative SP anomalies caused by the streaming potential as well as positive ones.

In the case of SP surveys in mountainous regions, we often observe terrain-related potentials or so-called topographic effect. Such potentials have negative correlations with topographic elevation, namely, the higher SP at the lower elevation. Namba (1939) experimentally investigated such terrain-related potentials and pointed out that the streaming potential associated with the ground water flow is a plausible cause. Ishido (1989) explained that such terrain-related potentials are caused by steady-state fluid flow due to spatial variations in the elevation of a water table. He theoretically pointed out that SP and topographic elevation should be linearly correlated with each other. However, it is not always the case in real fields. Gradient of SP per unit elevation change varies from place to place (in general, -0.1~-10mV/m). The variation of the topographic effect is considered to be caused by those of physical properties of the field such as the permeability and the electrical resistivity of the ground as well as the ion content in the permeating fluid. Estimation of the steady ground-water flow causing the terrain-related potentials and the reduction of the topographic effect is one of the unsolved problems in SP studies.

There are a few previous studies which dealt with the temporal variation of SP in association with volcanic activity. One of the examples is Zablocki (1976), which clarified that the amplitudes of positive SP anomalies corresponding to pit craters changed with volcanic activity. Nishida and Tomiya (1987) and Matsushima et al. (1990) investigated the temporal SP changes on Usu volcano, Japan, and evidenced that a positive SP anomaly covering the whole area of the summit crater has decayed with the subsidence of the volcanic activity after the eruption in 1977. Besides, on Piton de la Fournaise volcano, a dry fissure which was formed in the August 1992 eruption created a local but large SP anomaly (1500mV, 150m) which disappeared a few months later (Zlotnicki et al., 1994b). Although these results were striking, they were only based on repeated surveys and hence rather poor in time resolutions. To our knowledge there is no previous study which succeeded in detecting temporal SP changes accompanying volcanic activity with continuous records except Namba (1939) which observed temporal changes in the vertical component of SP accompanying explosive events of Aso volcano. Monitoring of SP with high time-resolution is required in order to detect a dynamic SP change within a few months associated with an eruption event.

1.2 Mechanisms of Self-Potential Generation

1.2.1 Electrokinetic Coupling

Fluid flow in a porous medium may generate an electric potential gradient along the flow path with the interaction between the moving pore fluid and the

electrical double layer (EDL) at the pore surface. The potential is called the electrokinetic or streaming potential.

At a solid-liquid interface, a complex electric charge distribution is formed. Among several possible models of the EDL, the Stern model is generally accepted. The Stern model of the electrical duoble layer is illustrated in Figure 1.1 (after Ishido and Mizutani, 1981). The potential on the surface of the solid phase (called surface potential), takes a negative value to the potential in the liquid phase. The Stern layer, which contains specifically adsorbed positive ions, exists next to the solid phase. Positive charges outer than Helmholtz plane diffusely spread out in the solution (Gouy diffuse layer). The plane at which shearing of the fluid flow begins is called the slipping plane, and the potential at the slipping plane referring to that in the normal solution is called ζ-potential. The ζ-potential takes a negative value when the specifical adsorption of positive ions is not significant in the Stern layer as in the case of Figure 1.1-(b). In ordinary conditions in the earth's crust, ζ-potential is negative.

The general relations between the electric current density $\boldsymbol{I}$, the fluid volume flux $\boldsymbol{J}$, the electric potential gradient gradϕ and the pore pressure gradient grad$\boldsymbol{P}$ are,

$$\boldsymbol{I} = -Lee \cdot \mathrm{grad}\phi - Lev \cdot \mathrm{grad}\boldsymbol{P} \quad , \quad (1.1)$$

$$\boldsymbol{J} = -Lve \cdot \mathrm{grad}\phi - Lvv \cdot \mathrm{grad}\boldsymbol{P} \quad , \quad (1.2)$$

where the Lxx are phenomenological coefficients. They can be described with the parameters of a capillary model as,

$$Lee = \eta t^{-2}\sigma = \eta t^{-2}(\sigma_f + \sigma_s / m) \quad , \quad (1.3)$$

$$Lev = Lve = -\eta t^{-2}\varepsilon\zeta / \mu \quad , \quad (1.4)$$

$$Lvv = k / \mu \quad , \quad (1.5)$$

where η is the porosity, t is the tortuosity of the capillary, σ_f and σ_s are the specific conductivity of the fluid in the capillaries ($\Omega^{-1} \cdot m^{-1}$) and the specific surface conductivity (Ω^{-1}), respectively, m is the hydraulic radius (m), ε and μ are the dielectric constant (F/m) and the viscosity (Pa · s) of the fluid in the capillaries, k denotes the permeability (m^2), ζ is the ζ-potential (V). The first term on the right-hand side in Eq. (1.1) represents Ohm's law and the second term in Eq. (1.2) represents Darcy's law. Besides, the term, -Lee · gradϕ corresponds to the conduction current, while the term, -Lev · grad$P$ does the 'conduction current' accompanying the fluid flow. In steady state equilibrium, the two terms are balanced by each other (Morgan et. al, 1989, Ishido and Kikuchi, 1987), and hence Eq. (1.1) results in Eq. (1.1'),

$$\text{grad}\phi = -C \cdot \text{grad}P \quad . \quad (1.1')$$

This is the steaming potential. The coefficient, C is called the streaming potential coefficient, and C=Lev／Lee=$\varepsilon\zeta/\sigma\mu$.

Ishido (1989) reviewed the theoretical studies on SP generation by Nourbehecht (1963), Fitterman (1978), and Sill (1983), and he classified the sources of SP generation into three types as is schematically illustrated in Figure 1.2:

TYPE I: sources result from fluid flow perpendicular to a boundary between regions with differing values of Lev (or the streaming potential coefficient, C)

TYPE II: a special case of TYPE I; the air-earth interface (ground surface) acts as a boundary (since Lev on the air is always zero)

TYPE III: sources associated with nonzero divergence of fluid flow

Sources of the conduction current are generated at the boundary of Lev or at the divergence of the fluid flow. In the case of a hydrothermal convection, possible sources of SP are those of TYPE I and TYPE II. Hence, SP anomalies accompanying the hydrothermal convection require the spatial inhomogeniety of Lev or the streaming potential coefficient. Many investigators have performed laboratory experiments on temperature and pH dependence (Ishido and Mizutani, 1981), permeability dependence (Jouniaux and Pozzi, 1995) of the streaming

potential coefficient and ζ -potential. In recent years, the property of the streaming potential by two-phase (vapor and liquid) flow is being clarified (Marsden, 1987; Antraygues and Aubert, 1993). These studies provide some bases of spatial inhomogeniety of the streaming potential coefficient.

1.2.2 Oxidation-Reduction Reactions

Sato and Mooney (1960) investigated the oxidation-reduction (redox) reactions associated with ore bodies. SP anomalies of this kind often accompany the ore bodies of pyrite, graphite, covellite, etc., and are in many cases negative in their polarities. Sato and Mooney (1960) pointed out the following conditons for the SP generation of this kind,

1) The ore body must be a good conductor of electricity (electronic rather than electrolytic conduction).
2) The ore must provide a nearly continuous connection between the ground waters of differing oxidation potential.
3) The ore must be chemically stable or inactive with respect to the oxidation potentials of the solutions with which it is in contact.
4) No permanent insulating films can form on the surface of the ore.

In general, the oxygen concentration of the ground water beneath the ground surface is higher than that at depth. Accordingly, the reaction,

$$O_2 + 4H^+ + 4e^- = 2H_2O \quad , \quad (1.6)$$

occurs in the shallow part, and at depth the reaction,

$$2H_2O = O_2 + 4H^+ + 4e^- \quad , \quad (1.7)$$

occurs. The ore body only plays a role of transporting electrons in itself and does not directly participate in the electrochemical reaction which yields self-potentials. In this way an oxygen concentration cell with the cathode at the top and the anode at the bottom of the ore is generated. The schematic illustration of the mechanism is shown in Figure 1.3. Sato and Mooney (1960) supposed that the largest anomaly caused by this mechanism is of the order of 400mV.

1.2.3 Electrochemical Concentration Cell

An electric potential is set up between two sections where there is a variation in the ion concentration of the soil. However, surveys cited by Corwin and Hoover (1979) showed that these electrochemical potentials should not exceed 20mV in ordinary geothermal areas. However, it is reported that an alunite field may indicate larger SP anomalies (Gay, 1967).

1.2.4 Thermoelectric Coupling

The thermoelectric coupling effect, a phenomenon which causes a voltage difference associated with a teperature gradient, is explained by the difference in speeds of the thermal diffusion of ions and electrons in the infiltrating fluid and rocks (Soret effect). A temperature gradient, gradT causes a corresponding voltage gradient, gradϕ:

$$\mathrm{grad}\phi = \boldsymbol{C} \cdot \mathrm{grad}\boldsymbol{T} \quad , \quad (1.8)$$

where $\boldsymbol{C}$ is called the thermoelectric coupling coefficient. The calculations performed on a buried spherical model in a two-layered earth by Nourbehecht (1963) and Corwin and Hoover (1979) showed that the maximun surface voltage is $0.15 \cdot (\boldsymbol{C}_1\text{-}\boldsymbol{C}_2) \cdot \triangle \boldsymbol{T}$, where $\boldsymbol{C}_1$ and $\boldsymbol{C}_2$ are thermoelectric coupling coefficients of the upper and lower layers, respectively, and $\triangle \boldsymbol{T}$ is the temperature difference between the sphere and its surroundings. For a value of $(\boldsymbol{C}_1\text{-}\boldsymbol{C}_2)$ of 1mV/℃, which is a large value given by laboratory experiments, the maximum potential corresponding to a $\triangle \boldsymbol{T}$ of 100℃ is 15mV.

1.3 Outline of the Thesis

Many investigators have dealt with basic problems of fluid flow or heat transfer in a porous medium. For example, Elder (1967) investigated the evolution of hydrothermal convection cells in a rectangular porous medium heated below. He discussed the start-up time of hydrothermal convection using his results of calculation. Carrigan (1986) theoretically dealt with a cooling process of shallow intrusion of magma and pointed out that two-phase flow which consists of vapor and hot ground water plays an important role in effective cooling of the magma. Active volcanoes are suitable fields to investigate such transient phenomena of subsurface hydrothermal systems.

The eruption of Unzen volcano, started in November 1990 leaving 198 years dormancy, kept on its activity for more than four years, and almost subsided

in May 1995. Total amount of the lava effusion was about 2×10^9 m^3. This eruption can be regarded as a suitable event series to investigate the evolution of a hydrothermal system including shallow ground water heated by magma which was set at a certain time. Direct detection of subsurface fluid flow is sometimes difficult to pursue, however. Meanwhile, the SP method is an indirect but effective technique to investigate such phenomena. A research group including the author conducted continuous observations and repeated surveys of SP around the active craters of Unzen volcano through almost all stages of the 1990-1995 eruption. Preliminary interpretations of the observations in the early stage were reported in Hashimoto and Tanaka (1995).

In this paper we try to investigate the hydrothermal system beneath Unzen volcano from spatial SP distributions and their temporal changes. The SP changes accompanying the 1990-1995 eruption can be mainly divided into three stages. Remarkable SP changes observed in each stage are explained by the movement or the intensity change of equivalent electric current sources. The physical meaning of these current sources is also discussed.

Section 2

A Brief Chronology of the 1990-1995 Eruption of Unzen Volcano

Unzen volcano (32°46' N, 130°18' E), an active stratovolcano, which consists of a group of dacitic lava domes, is located in the center of Shimabara peninsula in Kyushu, southwest Japan. The massif of the volcano extends approximately 20km and 25km in east-west and north-south directions, respectively including its skirts. The volcano has a horseshoe-shaped caldera open to southeast. Fugen-dake, the previous peak of Unzen volcano, is situated in the central part of the caldera, while Myoken-dake, Kunimi-dake, and Emaru-dake form a western part of the caldera rim as is shown in the topographic map of Figure 2.1. The southeastern part of the caldera rim is considered to have collapsed before the formation of Fugen-dake (Tanaka and Nakada, 1988). It has been revealed by geological studies that Unzen volcano has repeated lava-dome extrusions with pyroclastic flows in every 4000~5000 years (e.g., Watanabe and Hoshizumi, 1995). The amount of products in the present summit eruption starting in 1990 is much larger than those of the last two flank eruptions which occurred in 1663 and 1792.

A summarized time series of the eruption is shown in the left-hand side of

Figure 2.2. Features of the volcanic activity during the eruption period had changes with time. At first, precursory seismic activity preceded the summit eruption, then fumarole and ash ejection became dominant, and thereafter, effusion of lava started.

During November to December in 1989, a swarm of earthquakes, which preceded the eruption, occurred 15~20km below Tachibana bay, approximately 10km west of Fugen-dake. The hypocenters shallowed eastward to the west coast of Shimabara peninsula after July 1990 (Umakoshi et al., 1994). Isolated volcanic tremors also started at this time. On November 17, 1990, Fugen-dake started phreatic summit eruption at Jigoku-ato and Kujuku-shima craters leaving 198 years dormancy. Besides, Byobu-iwa crater started intensive ejection of dense volcanic ash on February 12, 1991. A lava dome appeared at the location of Jigoku-ato crater on May 20. Shallow earthquakes, severe ground deformations, and some explosive events preceded the appearance of the dome. The dome, effusing and collapsing lava, gradually grew itself. The dome at first showed exogenous growth, which is characterized by recurrent process of effusion and collapse of lava. However, endogenous growth accompanied by remarkable ground deformations became dominant after December 1993 (Kyushu univ. et al, 1994).

A temporal change of effusion rate is shown in the right-hand side of Figure 2.2 (after Nakada and Shimizu (1995)). There were two pulses of magma supply; the first pulse lasted from May 1991 to January 1993, and the second one from February 1993 to early 1995 (Nakada and Shimizu, 1995).

Approximately ten thousand Merapi-type pyroclastic flows occurred since the appearance of the lava dome till the subsidence of the eruption in 1995 (Nakada and Shimizu, 1995). Effusion of lava almost stopped in early 1995 and the volcanic activity progressively receded thereafter.

Section 3

MEASURING SYSTEMS

A research group including the author started SP observations in the summit area of Unzen volcano in March 1991, two months before the first extrusion of a lava dome. The site distribution of SP measurements is shown in Figure 3.1. The sites for continuous observations are denoted by letters (A-G) in Figure 3.1. Stations B, C, D, E, and F were installed on March 20, 1991. Stations A and G were added on August 3, 1991 and March 12, 1992, respectively. Repeated surveys were carried out approximately once a month at the sites denoted by solid circels in Figure 3.1. Reliable data of the repeated surveys are available after Decemeber 1991. The sampling interval of the continuous observations was 40 minutes. Although the survey area was free from the noise of AC power lines, the 22.2kHz electromagnetic noise was severe because the VLF station for submarine communications is located in Miyazaki prefecture (about 150km SSE from Unzen). Hence passive low-pass filters were inserted at each input of the data logger placed at the site B to avoid the aliasing.

Electrodes of the Pb-$PbCl_2$ type were used for both repeated surveys and continuous observations. The electrodes were wrapped with clay and buried at the depth of 0.3~0.5m to minimize anomalous potential changes at the electrode-

earth interface by rainfall. The Pb-$PbCl_2$ electrode used here consists of a lead wire and the powder of lead-chloride packed in a porous cup. This type of electrode is maintenance-free and suitable for a long-term observation since it consists of only solid materials (Electrodes with electrolytic solutions need a periodic maintenance). However, the stability of the electrode was unknown. To check this point, we sometimes measured potential difference between the Pb-$PbCl_2$ electrodes (buried) and a Cu-$CuSO_4$ electrode (portable) at each site. The potentials of a Pb-$PbCl_2$ electrode referred to a Cu-$CuSO_4$ electrode were, in most cases, in the range of -450mV~-500mV.

Section 4

Results of Self-Potential Observations

Equipotential maps of SP in December of 1991, 1992, 1993, and 1994 are shown in Figure 4.1-(a), (b), (c), and (d), respectively. The most significant SP change was observed around the first extrusion of the lava dome in May 1991. The SP change accompanying the dome extrusion will be discussed in detail in a later section. Although noticeable temporal SP changes were detected after the first extrusion of the dome, basic features of spatial SP distributions did not change significantly through all stages of the eruption. Namely, all the SP maps in Figure 4.1 have in common three positive SP regions (H1, H2, and H3) and one negative SP region (L1). As has been pointed out in Hashimoto and Tanaka (1995), H1 and H2 are terrain-related potentials (in general, higher SP at lower topographic elevation). Meanwhile, a positive SP (H3) which lies in the vicinity of the lava dome can be attributed to the streaming potential caused by subsurface hydrothermal upwelling. As is recognized in Figure 4.1, the negative region L1 had changed its intensity and location with time. The temporal change of L1 will be discussed later in detail.

Time series of SP at the sites 15 and D are shown in Figure 4.2. The SP changes detected in the summit area of Unzen can be divided into two distinct

types, namely, those in the northern sites (typically observed at the site 15, the upper panel of Figure 4.2) and those in the southern sites (typically observed at the site D, the lower panel of Figure 4.2). As is discussed later, the periods during which characteristic SP changes occurred seem to coincide with those during which severe local ground deformations near the dome occurred. Here we divide the 1990-1995 eruption period of Unzen volcano into three stages noting the relationship between SP changes and the activity of the lava dome.

The first stage covers approximately two months from the late March through June 1991, which corresponds to the period from the beginning of observation to one month after the appearance of the lava dome. A steep rise in SP at southern sites was detected in this period by continuous record (unfortunately there was no observation at northern sites in this period).

The second stage covers two and a half years from June 1991 to December 1993, during which the lava dome erupted in an exogenous manner. The trend of increase at southern sites changed remarkably after the first dome extrusion. For instance, the trend of increase at the site D in the first and the second stages are approximately 5.7mV/day and 0.2mV/day, respectively. Besides, we can recognize decreases in SP at northern sites in the second stage. The trend of SP change at the site 15, which showed the most significant decrease, is about -1.4mV/day.

The third stage originates from January 1994, after which the manner of dome growth became endogenous and the volcanic activity progressively receded. In this period, self-potentials at southern sites continued to increase at first with

their trends getting rather steep again, then almost stopped to increase after 1995. Meanwhile, SP at northern sites reversed into increase at first, and then, almost ceased their changes likewise after 1995. The three stages described above are indicated by numbers with circles in the two panels of Figure 4.2.

Section 5

Hydrothermal System Inferred from Self-Potential

The electric streaming potential is caused by selective ion transport with fluid flow along a solid-liquid interface in a porous medium (in ordinary conditions in the earth's crust, positive charges are transported with fluid flow). A pair of conductive electric current sources in positive and negative signs appear at the region where the streaming potential coefficient (efficiency of charge transport) effectively decreases and increases along a flow path, respectively (Ishido, 1989). There are some causes of the change in the streaming potential coefficient. The following two are important in the case of a hydrothermal system. One is a temperature change along a flow path. Magnitude of the streaming potential coefficient and the temperature of the system are positively correlated (Ishido and Mizutani, 1981). The other is the fluid flow crossing the ground surface. The electrokinetic phenomena do not occur and hence the streaming potential coefficient is zero above the ground surface. In this case, the ground surface works as a boundary.

Considering these facts, we can infer that steam flow in the fumarolic area of a volcano transports positive electric charges toward the ground surface. The electric charges will be stagnant beneath the ground surface because of temperature

decrease or dissipation of carrier fluid into the atmosphere across the ground surface. Besides, negative charges balancing positive ones should be distriburted somewhere in the system for charge neutrality. As a consequence, electric conduction current is generated according to the charge distribution. In a steady state, the conduction current should be balanced with the current by the charge transfer with fluid flow. The distribution of excess charges results in corresponding SP anomalies on the ground surface. In the case of fumarole ejection, negative charges (or current sources) should be distributed around where the upward fluid flow originates, e.g., where magma heats up surrounding ground water. If they are situated in a sufficiently large depth, a positive SP anomaly observed on the ground surface can be approximately explained by only a positive current source in the shallow part. However, this approximation is not valid in the case that the depth of a negative source is comparable to that of a positive source; both sources are necessary to explain the SP distribution.

In general, raw SP profiles measured on the ground surface contain some kinds of noises such as terrain-related potentials, regional background anomalies affected by geological inhomogeneity, and so on. Hence, we should remove these noises in order to make clear the effect of the streaming potential accompanying volcanic activity. Some investigators adopt the first-order correction for topographic effect by assuming a constant SP gradient versus topographic elevation throughout the survey area. However, such kind of topographic correction is not always valid in the field with strong heterogeneity in geophysical conditions such as the permeability, the elecrical resistivity, and

so on. In the case of Unzen, the topographic effect is -7~-10mV/m around H1, H2 in Figure 4.1. Simple topographic correction with such a large coefficient may mask other small SP anomalies. To evade this problem, we only treat the differences of two SP maps in the following subsections 5.2 and 5.3. Assuming background anomalies do not change with time, we can extract SP changes related to volcanic activity through this process. Let us consider the three stages of observed SP changes described above according to this point of view.

5.1 First Stage *(late March through June 1991: growth of hydrothermal upwelling accompanying magma ascent)*

The first stage can be interpreted as an ascending process of a positive electric current source with the magma head as shown in Figure 5.1-(a). Let us see the temporal change of SP profiles along the path from the lava dome toward the southwest direction. Monthly averaged values at each continuous observation site (B-G) were plotted versus the horizontal distances between each site and former-Jigoku-ato crater (or the lava dome) in the upper panel of Figure 5.2. A profile of topographic elevation is also shown in the lower panel of Figure 5.2. We can recognize the SP is higher toward the lava dome, the topographic height. The topographic effect of SP is generally results in lower potentials toward a summit. Hence the results in Figure 5-2 imply a positive SP anomaly at the dome. In addition, we can recognize that the SP has increased remarkably around the site E with time in this period. These facts imply the

existence of a positive SP anomaly centered at the active craters (lava dome) before the dome extrusion, and suggest the generation of a positive current source under the site E accompanying the magma ascent in the first stage.

Magneto-Telluric surveys conducted by Joint University Research Group have revealed that an aquifer exists widely below Shimabara peninsula at the depth between -1.0km to +0.5km above sea level (JURG, 1992). Considering the fact of mixing of much meteoric water in fumaroles before the appearance of the lava dome (isotope analysis of volcanic gases by Hirabayashi, pers. commun.), fumaroles in the first stage are supposed to have contained much ground water in the aquifer. Accordingly, we consider that negative current sources were fixed around -1.0km, the depth of the lower level of the aquifer, where the upward hydrothermal fluid flow seems to have originated from; meanwhile, a positive current source corresponding to the high temperature zone, which effectively transport positive charges, ascended with the magma head.

5.2 SECOND STAGE *(June 1991 to December 1993: establishment of shallow hydrothermal convection)*

The main feature of SP changes in the second stage is the increase at southern sites and the decrease at northern sites. This corresponds to a gradual northward movement of the low SP region, L1, and its intensifying in magnitude in Figure 4.1. Here in Figure 5.3-(a) we show the distribution of the difference between two equipotential maps of SP, regarding the one in December 1991,

which is shown in Figure 4.1-(a), as a virtual initial condition of the second stage (, though it must be better to take the spatial distribution of SP in June 1991 as a virtual initial phase of the second stage, if it were available).

As is recognized in Figure 5.3-(a) the SP decrease in the second stage seems to have occurred around the site 15 (0.5km west of the dome) with the extent of approximately 500m in diameter. The maximum decrease in this period amounted to -500mV. On the other hand, SP increase seems to have occurred around the southwest of the lava dome. The maximum increase observed in the second stage was +300mV. The extent of SP increasing zone is not clear because the contours in this period do not close by themselves. However, if we regard the area of higher than +200mV as the southwestern half of the SP increasing zone, its scale is comparable to that of the decreasing zone mentioned above.

The second stage is considered as the period of establishment of a shallow hydrothermal convection involving peripheral ground water which was gradually heated by the magma having intruded in the first stage. After the shallow intrusion of magma, quasi-steady thermal supply from magma is supposed to have heated up the peripheral ground water and driven upward fluid flow. The upwelling near the heat source might have resulted in descending flow of ground water for supplying the permeating fluid toward the fumarolic area from surroundings. As is illustrated in Figure 5.1-(b), positive electric current sources might have appeared at the end of the convective fluid flow, while negative sources done at the start point of the flow. The upward flow near the heat source and downward flow in the peripheral area explain the SP increase at the southwest of the dome and the

SP decrease near the site 15, respectively.

5.3 THIRD STAGE *(January 1994 to 1995: lateral expansion of upwelling area)*

In Figure 5.3-(b) we show the distribution of the difference between Figure 4.1-(c) and (d) in order to see the SP change in the third stage in the same way we did in the second stage. The third stage is characterized by endogenous growth of the lava dome with remarkable ground deformations (Geological Survey of Japan and Unzendake Weather Station, JMA, 1995), which implies a shallow ground dilatation. The endogenous growth occurred under the condition of a vent choked with viscous magma. Then the magma beneath the ground surface pushed the lava dome looking for its exits. SP changes on the ground surface showed concentric increase with its center at the southwest part of the dome as was shown in Figure 5.3-(b). The expansion of high SP region can be attributed to that of upwelling area of thermally driven ground water or volatilized steam. This situation is illustrated in Figure 5.1-(c).

Section 4
DISCUSSION

6.1 Location of Downflow

There is a plausible reason for the local SP decrease in the second stage. The region which showed SP decrease in the second stage was located between the western rim of Myoken caldera and the peak of Fugen-dake, and the site 15 is located on a resistivity boundary lying in north-south direction. This resistivity boundary was detected by some kinds of resistivity surveys performed in the summit area of Unzen after the eruption. For instance, results of an air-borne electromagnetic survey by Mogi et al. (1995) indicate that the western rim of Myoken caldera (Kunimi-dake and Myoken-dake) is more resistive and hence less permeable than surroundings. This result is also supported by the apparent resistivity map of DC electric soundings (dipole mapping method) by the author which is shown in Figure 6.1.

From geological viewpoint, Fugen-dake is considered to have been formed later than Myoken-dake and Kunimi-dake (Tanaka and Nakada, 1988). A geological map indicates that Fugen-dake erupted penetrating Myoken-dake lava. Besides, the upper level of a water-bearing layer in the shallow part of Fugen-dake is considered to be 100-200m in depth as shown in the schematic picture of

Figure 6.2. The bases of such a structure are provided by the layer resistivity structure deduced from the air-borne EM survey (Mogi et al., 1995) and vertical DC electric soundings with Schlumberger array which were conducted by the author. Downward flow of the ground water caused by a hydrothermal convection is considered to have originated at this depth because a pressure change associated with heat-up cannot reach above the upper level of the water-bearing layer. Consequently, it is reasonable to suppose a negative current source under the site 15.

6.2 Comparison to Other Observations

Time series of the ground deformation (slope distance measured by EDM; Geological Survey of Japan and Unzendake Weather Station, 1995) and the geomagnetic total force observed with proton magnetometers (Tanaka et al., 1995) are shown in Figure 6.3 with those of the self-potentials. Significant changes in geomagnetic total force and ground deformations are recognized around May 1991 and December 1993. It is noteworthy that these two periods correspond almost to those of remarkable SP changes. Tanaka et al. (1995) explained the geomagnetic changes in the former period by the effect of replacement of magnetized igneous rocks by nonmagnetic magma body which intruded to the shallow part. As for the changes in the latter period (December 1993), Tanaka et al. (1995) proposed a model of an equivalent demagnetized sphere close to the ground surface at approximately 200m west from the lava dome. They pointed out that the thermomagnetic effect is one of the most

important mechanisms for the geomagnetic changes in which hydrothermal fluid motion is a dominant process of heat transfer in the subsurface. On this viewpoint, it is natural to consider that the change in the manner of growth of the lava dome strongly affected the heat transfer in the shallow subsurface. Namely, under the capped condition of the dome, upwelling area of the hydrothermal fluid or hot volcanic gases expanded looking for a way out, and consequently, caused the thermal demagnetization of peripheral igneous rocks. This idea supports the author's fluid flow model in the third stage.

The pattern of lava effusion in the third stage is supposed to be similar to that in the first stage on a point that the upper part of the magma vent was obstructed by rocks or viscous lava. Features of SP changes in the two stages are also similar to each other in a point that their centers of increase are both located in the southwestern part of the lava dome. This leads us to an idea that a fracture or a steam vent exists in the shallow subsurface under the southwestern part of the dome. Volcanic gases or hot steam might have been ascended along the fracture when the main outlet was capped with viscous lava.

6.3 Other Possible Causes of SP Generation

Self-potential change is also produced by other processes besides the streaming potential. Several mechanisms have been proposed for the cause of negative SP anomalies on the ground surface such as the effect of the electrochemical concentration cells, the oxidation-reduction reaction, the thermoelectric coupling, and so on. However, the amount of the SP decreases in

the second stage is large enough to exclude the possibility of the effect of the electrochemical concentration cells (The mechanism cannot produce potential difference larger than a few tens of millivolts. (Corwin and Hoover, 1979)). Thermoelectric coupling cannot be adopted because there was no local anomaly in ground temperature around the SP decreasing area in the second stage. It is the oxidation-reduction process that cannot be ignored in this case. For instance, changes in the contents of aqueous solution caused by mixing of volcanic acid gases into local ground water might have caused a local negative SP anomaly (Massenet and Pham, 1985). To our present knowledge, however, there is no positive basis enough to assume the local mixing of volcanic gases into the subsurface of the SP decreasing region.

6.4 Future Works

In this paper, we explained the observed SP changes by qualitative models of electric current sources. A quantitative approach by calculations of equivalent current sources and corresponding fluid flow is one of the future works which will bring a viewpoint of volcano-hydrology and the energy-budget study in the eruption event.

The electrodes used in this study worked well in the field of Unzen because the SP changes associated with the volcanic activity were enough large. However, it needs further improvements in accuracy and long-term stability of electrodes to investigate the fields which show weaker SP anomalies.

It has been often emphasized in recent years that ground water existing

beneath a volcano can affect the eruption style and also has an important role for various kinds of precursor phenomena of an eruption. For instance, Kagiyama (1995) maintained that many kinds of phenomena accompanied by volcanic eruption can be explained by the relationship between the depth of water-bearing layer and the magma head. He also pointed out that the differences in eruption style in some volcanoes can be attributed to the exsitance (or non-exisitance) of aquifer beneath the volcanic edifice. Therefore, the SP observation, as an indicator of subsurface fluid flow in volcanoes, will be one of the effective methods in monitoring volcanic activity.

Section 7

CONCLUSIONS

The electric self-potential in association with the 1990-1995 eruption of Unzen volcano was investigated. A distinct positive SP anomaly and a neighboring negative anomaly were observed on the volcano. Besides, temporal variations of these anomalies were detected through continuous observations and repeated surveys. Then a hydrothermal system beneath the volcano was deduced from the SP data according to the streaming potential theory. The eruption period can be divided into three distinct stages with reference to the SP changes, and each stage may be characterized by the different phase of the evolution process of a hydrothermal system. Namely, the hydrothermal upwelling with magma ascent in the first stage, the establishment of a shallow hydrothermal convection in the second stage, and the expansion of the upwelling area around the lava dome in the third stage.

REFERENCES

Antraygues, P. and M. Aubert, Self Potential Generated by Two-Phase Flow in a Porous Medium, Experimental Study and Volcanological Applications, J. Geophys. Res., 98, 22273-22281, 1993.

Carrigan, C. R., A Two-Phase Hydrothermal Cooling Model for Shallow Intrusions, J. Volcanol. Geotherm. Res., 28, 175-192, 1986.

Corwin, R. F. and D. B. Hoover, The self-potential method in geothermal exploration, Geophysics, 44-2, 226-245, 1979.

Elder, J. W., Transient convection in a porous medium, Jour. Fluid Mech., 27, 609-623, 1967.

Fitterman, D. V., Electrokinetic and Magnetic Anomalies Associated With Dilatant Regions in a Layered Earth, J. Geophys. Res., 83, 5923-5928, 1978.

Gay, S. P., Jr., A 1,800 Millivolt Self-potential Anomaly Near Hualgayoc, Peru, Gephys. Prosp., 15-2, 236-245, 1967.

Geological Survey of Japan and Unzendake Weather Station, JMA, Ground Deformation of Fugen-dake, Unzen Volcano, measured by EDM between June 1994 and October 1994 (in Japanese), in Rep. of Coordinating Committee for Prediction of Volcanic Eruption, 60, pp.99-106, 1995.

Hashimoto, T. and Y. Tanaka, A large self-potential anomaly on Unzen Volcano, Shimabara peninsula, Kyushu island, Japan, Geophys. Res. Lett., 22-3, 191-194, 1995.

Ishido, T., Self-potential generation by subsurface water flow through electrokinetic coupling, in detection of subsurface flow phenomena, Lecture Notes in Earth Sciences 27, 121-131, Springer-Verlag, 1989.

Ishido, T., Subsurface fluid flow inferred from self-potential distribution in volcanic areas, Transactions of 1991 meeting of Conductivity Anomaly Research Group, 86-93, 1991.

Ishido, T. and T. Kikuchi, The Self-Potential Method, Geothermal Energy, 12, 425-443, 1987.

Ishido, T. and H. Mizutani, Experimental and theoretical basis of electrokinetic phenomena in rock-water systems and its applications to geophysics, J. Geophys. Res., 81, 1763-1775, 1981.

Ishido, T., T. Kikuchi, Y. Yano, M. Sugihara, and S. Nakao, Hydrogeology inferred from the self-potential distribution, Kirishima geothermal field, Japan, Geothermal Resources Council Transactions, vol.14, 919-926, 1990.

Joint University Research Group (Geophysical Party), Geophysical Observation of the 1990-1992 Eruption at Unzen Volcano (Part1) (in Japanese), Bull. Volcanol. Soc. Japan, 37-4, 209-215, 1992.

Jouniaux, L. and J. P. Pozzi, Permeability dependence of streaming potential in rocks for various fluid conductivities, Geophys. Res. Lett., 22, 485-488, 1995.

Kagiyama, T., Volcanological significance of resistive layer in volcanic area (in Japanese), Transactions of 1995 meeting of Conductivity Anomaly Research Group, 106-111, 1995.

Kyushu University, Earthquake Research Institute, University of Tokyo, and Geological Party of the Joint University Research Group, Geological Report of Eruption at Unzen Volcano During June-October 1994 (in Japanese), in Rep. of Coordinating Committee for Prediction of Volcanic Eruption, 60, pp.119-130, 1994.

Marsden, S. S., Two phase streaming potentials, in Proc. 12th workshop on geothermal reservoir engineering, Stanford univ., pp.147-151, 1987.

Massenet, F. and V. N. Pham, Mapping and Surveillance of Active Fissure Zones on a Volcano by the Self-Potential Method, Etna, Sicily, Jour. Volc. Geotherm. Res., 24, 315-338, 1985

Matsushima, N., M. Michiwaki, N. Okazaki, R. Ichikawa, A. Takagi, Y. Nishida, and H. Y. Mori, Self-Potential Studies in Volcanic Areas (2) -Usu, Hokkaido Komaga-take and Me-akan-, Jour. Fac. Sci., Hokkaido Univ., Ser.VII (Geophysics), 8-5, 465-477, 1990.

Mogi, T., Y. Tanaka, T. Morikawa, K. Kusakabe, M. Tanahashi, T. Nakatsuka, K. Tanaka, and H. Utada, Subsurface Structure of Unzen-Fugen and Mayuyama Volcano Inferred from Airborne Electromagnetic Method and Magnetic Survey (in Japanese), Bull. Volcanol. Soc. Japan, 40, 263-276, 1995.

Morgan, F. D., E. R. Williams, and T. R. Madden, Streaming potential properties of Westerly granite with applications, J. Geophys. Res., 94, 12449-12461, 1989.

Nakada and Shimizu, The 1991-1994 Activities of Unzendake Volcano, in Reports

on Volcanic Activities and Volcanological Studies in Japan for the Period from 1991 to 1994, presented at the XXI General Assembly of IUGG in Boulder, Colorado, pp.2-9, 1995.

Namba, M., An investigation of the earth-current on the volcano Aso, Dr. thesis, Kyoto univ., 1939.

Nishida, Y. and H. Tomiya, Self-potential studies in volcanic areas (1) -Usu volcano-, Jour. Fac. Sci., Hokkaido Univ., Ser.VII (Geophysics), 8-2, 173-190, 1987.

Nourbehecht, B., Irreversible thermodynamic effects in inhomogeneous media and their applications in certain geoelectric problems, Ph. D. thesis, M. I. T., 1963.

Sill, W. R., Self-potential modeling from primary flows, Geophysics, 48, 76-86, 1983.

Sato, M. and H. M. Mooney, The electrochemical mechanism of sulfide self-potentials, Geophysics, 25, 226-249, 1960.

Tanaka, M. and S. Nakada, Geology of eastern part of Unzen Volcano, The Sci. Rep. Shimabara Earthquake and Volcano Observatory, Fac. Sci., Kyushu Univ., 14, 1-11, 1988.

Tanaka, Y., H. Masuda, T. Hashimoto, H. Utada, Y. Sasai, and T. Kagiyama, The volcanic activity of Unzendake inferred from geomagnetic changes, in report of research project grant-in-aid for scientific research (A) 06306011, 14-21, 1995.

Umakoshi, K., H. Shimizu and N. Matsuwo, Magma Ascent Path in the 1990-94

Eruption of Fugendake, Unzen Volcano, as inferred from Precisely Determined Hypocentral Distribution (in Japanese), Bull. Volcanol. Soc. Japan, 39-5, 223-235, 1994.

Watanabe, K. and H. Hoshizumi, Geological map of Unzen volcano, Geological Survey of Japan, 1995.

Zablocki, C, J., Mapping thermal anomalies on an active volcano by the self-potential method, Kilauea, Hawaii, in Proceedings of the 2nd U.N. Symposium on the Development and Use of Geothermal Resources, vol.2, pp.1299-1309, U.S. Government Printing Office, Washington, D.C., 1976.

Zlotnicki, J., M. Feuillard, and G. Hammouya, Water Circulations on La Soufriere Volcano Inferred by Self-Potential Surveys (Guadeloupe, Lesser Antilles). Renew of Volcanic Activity?, J. Geomag. Geoelectr., 46, 797-813, 1994a.

Zlotnicki, J., S. Michel, and C. Annen., Anomalies de polarisation spontanee et systems convectifs sur le volcan du Piton de la Fournaise (Ile de la Reunion, France), C. R. Acad. Sci. Paris, 318, 1325-1331, 1994b.

Zohdy, A. A. R., L. A. Anderson, and L. J. P. Muffler, Resistivity, self-potential, and induced-polarization surveys of a vapor-dominated geothermal system, Geophysics, 38, 1130-1144, 1973.

Figure Captions

Figure 1.1 (a)The Stern model of the electrical double layer. (b)The potential variation according to the Stern model (in the Stern layer the potential varies linearly). (c)The potential variation when the Stern layer contains more (positive) charges than is required to balance the (negative) charges on the solid. (after Ishido and Mizutani, 1981)

Figure 1.2 Three types of electric conduction current sources important for electrokinetic coupling in subsurface water flow problems. (after Ishido, 1989)

Figure 1.3 A schematic illustration of an electrochemical mechanism for self-potentials. (after Sato and Mooney, 1960)

Figure 2.1 Location and topography of Unzen Volcano. Topographic ridges are emphasized by thick broken lines and valleys by thin broken lines. Height is represented in meters.

Figure 2.2 A time series showing the volcanic activity of Unzen. The meshed bars represent the period of activities of J (Jigoku-ato), K (Kujuku-shima), and B (Byobu-iwa) craters. Three stages of the self-potential changes are according to the description in the section 4. The effusion

rates of lava are after Nakada and Shimizu (1995).

Figure 3.1 Distribution of observation sites. Repeated survey points are denoted by solid circles, while continuous observation sites by open ones. Broken lines show the traces of extra-surveys which were also used in making the equipotential maps of SP in Figure 4.1.

Figure 4.1 Self-potential distributions in December of (a) 1991, (b) 1992, (c) 1993, and (d) 1994. Potentials of each SP map are referred to Nita pass (a dot in a circle) and are indicated in millivolts. Results of extra-surveys (broken lines in Figure 3) have been also compiled in these maps.

Figure 4.2 Temporal variations of SP at the site 15 and the site D as representatives of the northern-type change and the southern-type change. Solid circles indicate the SP measured with Pb-$PbCl_2$ electrodes, while open rectangles with Cu-$CuSO_4$ electrodes. Numbers in circles represent the stages 1, 2, and 3 which are divided by vertical thick solid lines.

Figure 5.1 Schematic illustrations of east-west cross sections showing equivalent electric current sources associated with fluid flow in (a) the first stage, (b) the second stage, and (c) the third stage.

Figure 5.2 Monthly averaged SP profiles (upper panel) and topographic elevation along the path crossing the sites B-G' in Figure 3 (lower panel). The horizontal axis is the distance between each site and the center of the former Jigoku-ato crater. The potential at the site B is assumed to be fixed.

Figure 5.3 Spatial distribution of SP changes (a) in the second stage and (b) in the third stage.

Figure 6.1 A map of the total apparent resistivity by dipole mapping measurements conducted in May and June 1995 indicating a north-south resistivity boundary crossing Fugen-dake.

Figure 6.2 A cartoon of a NW-SE cross section illustrating the generation mechanism of a negative SP anomaly around the site 15. Arrows indicate the flow of ground water. The resistivity structure is based on the results of the air-borne EM survey (Mogi et al., 1995) and the DC electric soundings performed by the author in 1994.

Figure 6.3 Time series showing the ground deformations (slope distance measured with EDM; after Geological Survey of Japan and Unzendake Weather Station, JMA, 1995) (top panel), and the geomagnetic total force with proton magnetometer (after Tanaka et al., 1995) (second panel), and

the self-potentials at the sites 15 (third panel) and D (bottom panel).

Figure 1.1
Figure 1.2

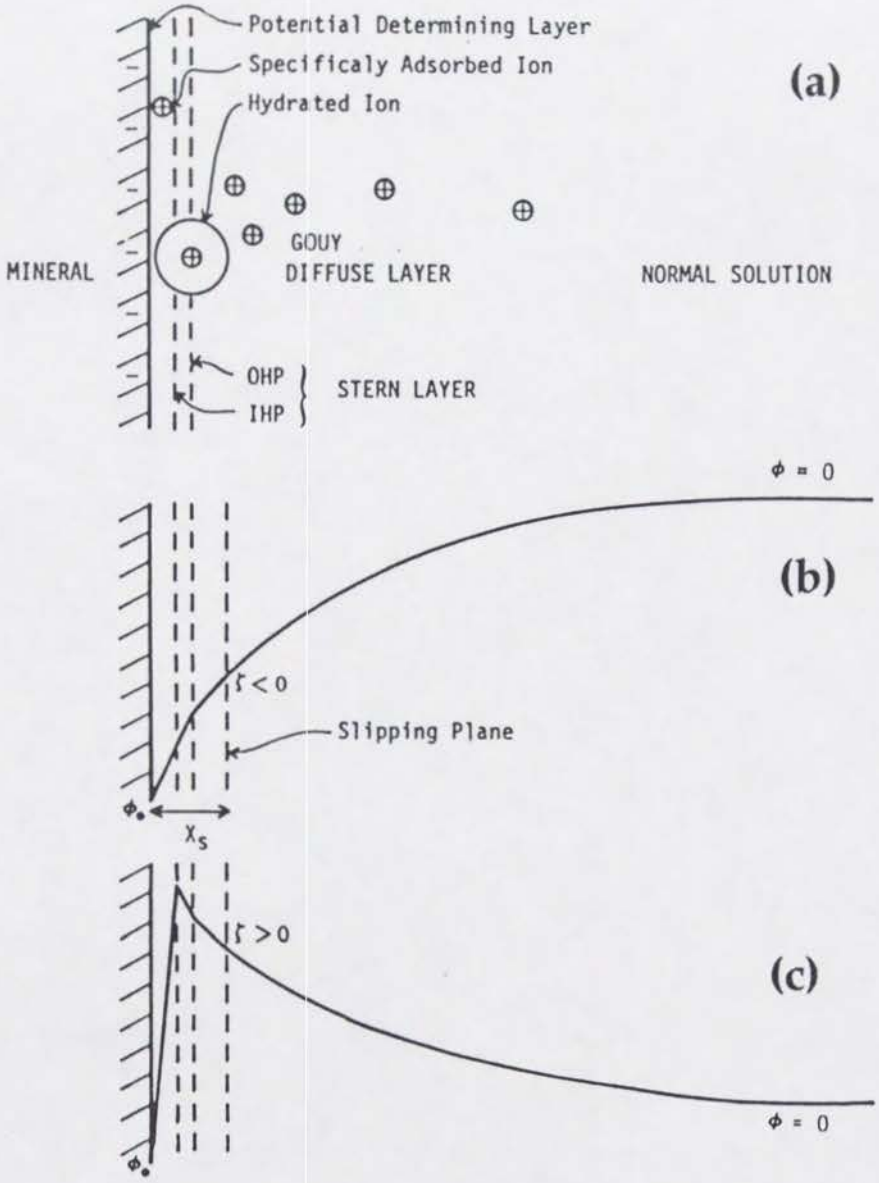

Figure 1.1

Figure 1.2

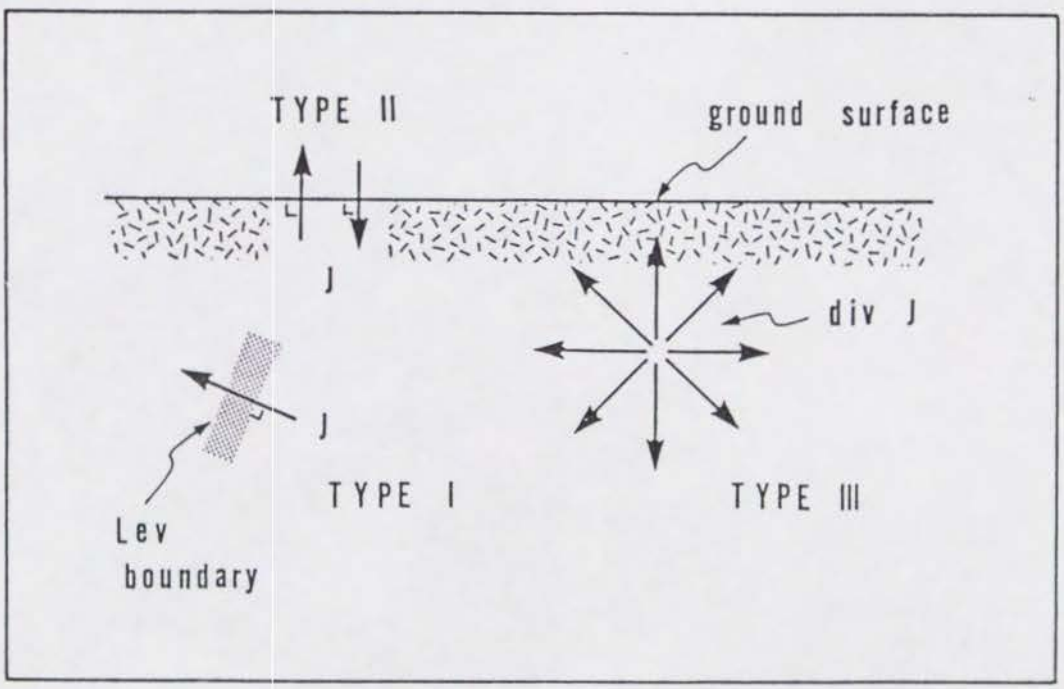

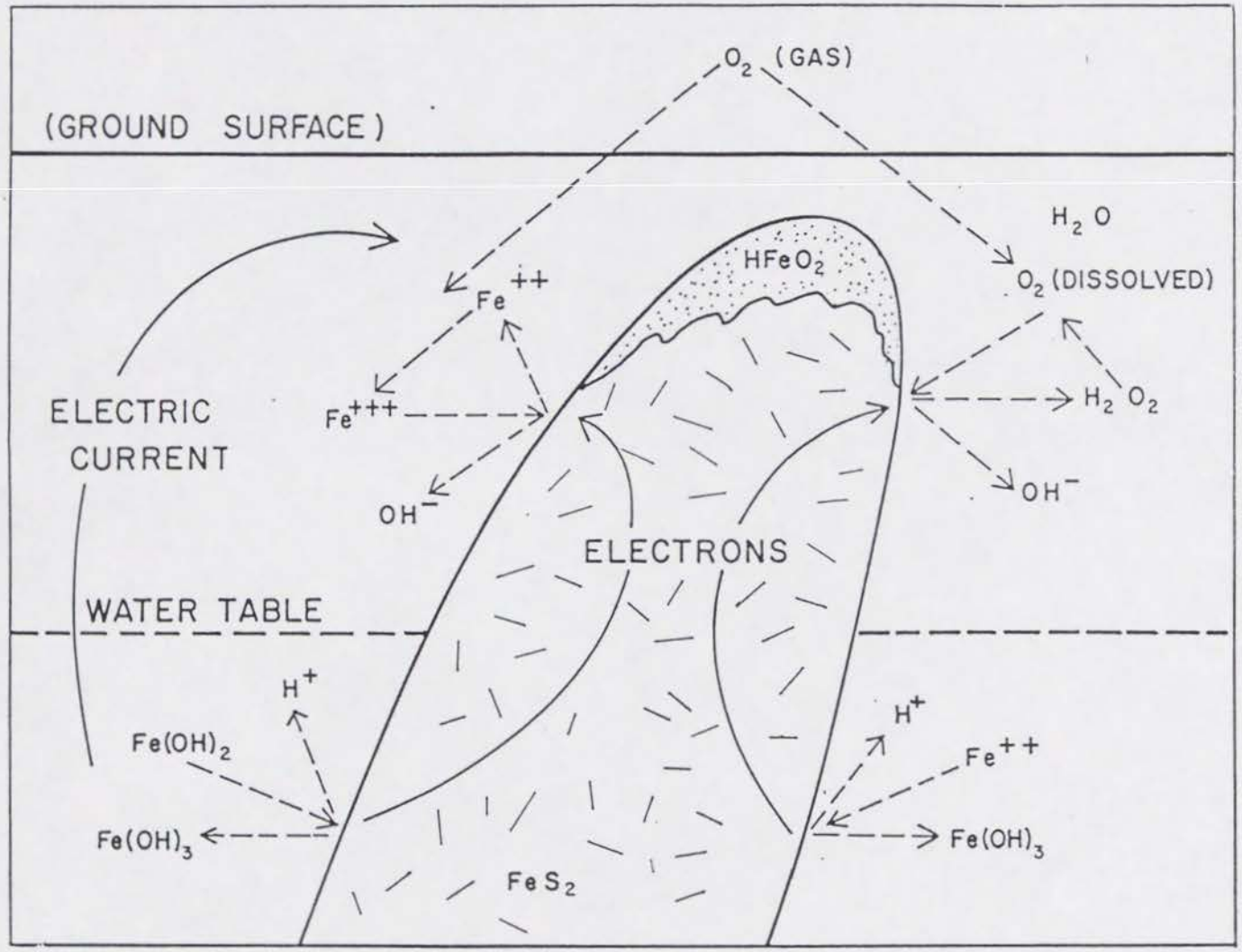

Figure 1.3

Figure 1.3

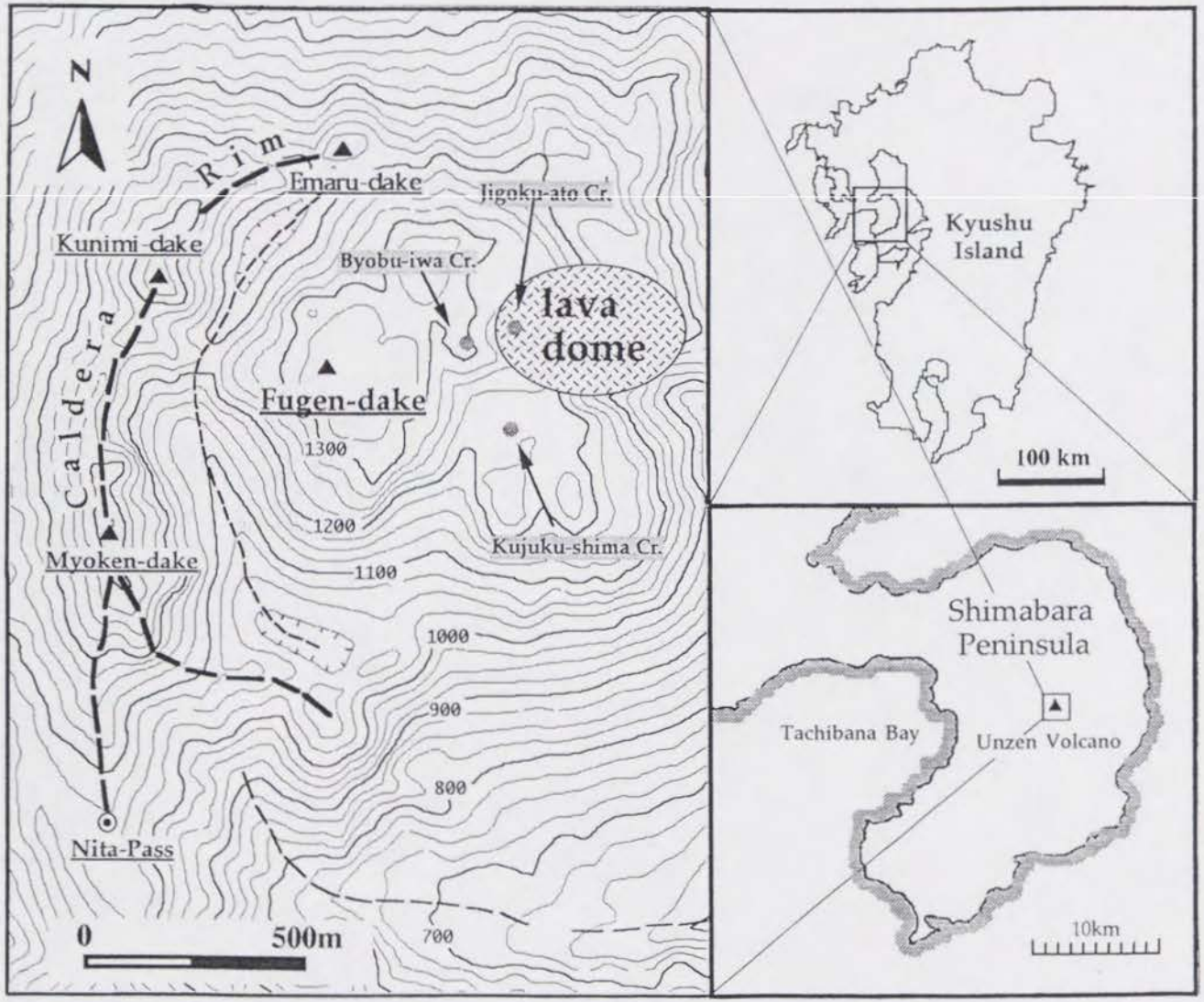

Figure 2.1

Figure 2.1

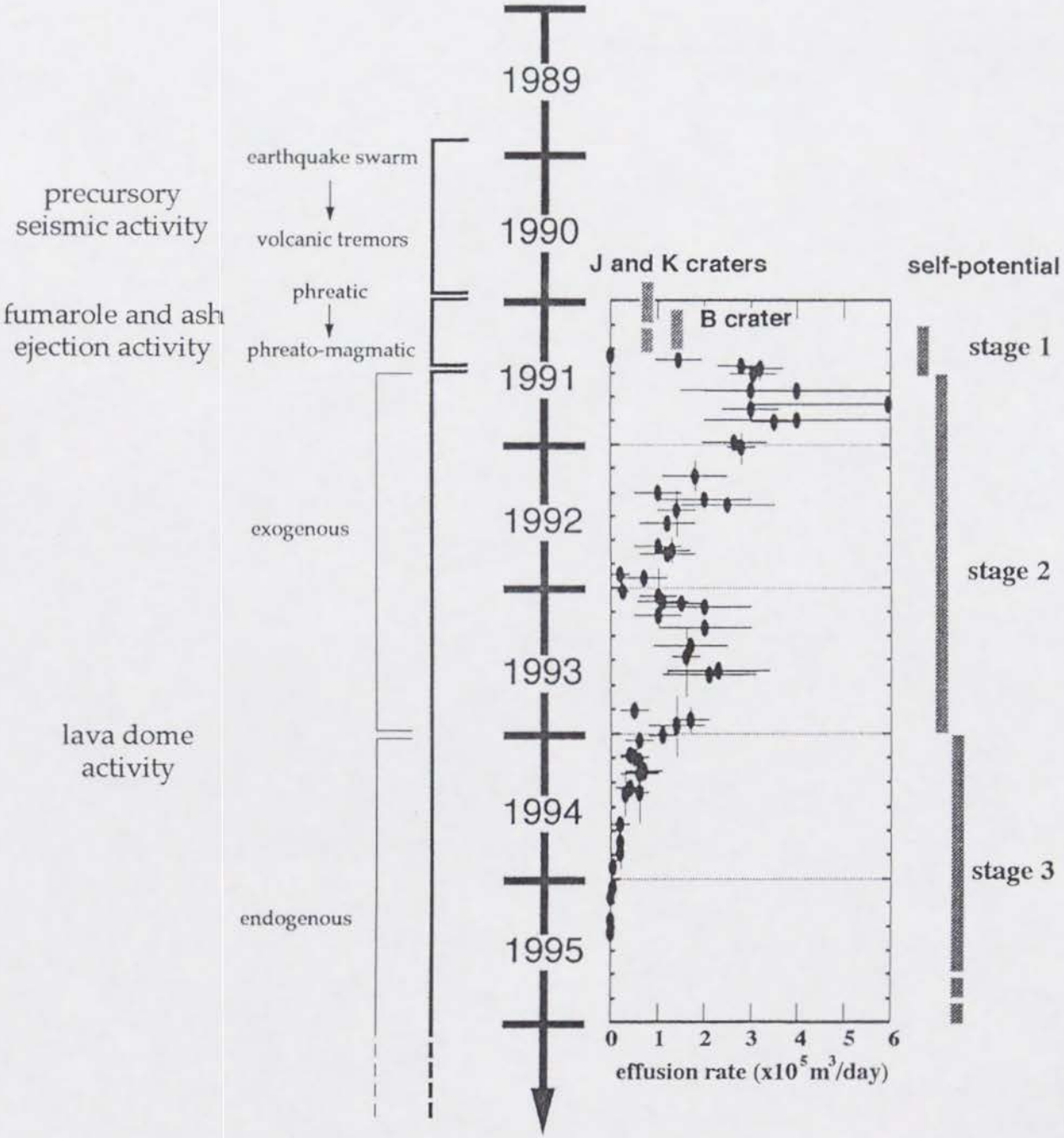
precursory seismic activity
fumarole and ash ejection activity
lava dome activity
earthquake swarm
volcanic tremors
phreatic
phreato-magmatic
exogenous
endogenous
1989
1990
1991
1992
1993
1994
1995
J and K craters
B crater
self-potential
stage 1
stage 2
stage 3
0 1 2 3 4 5 6
effusion rate (x10^5 m^3/day)

Figure 2.2

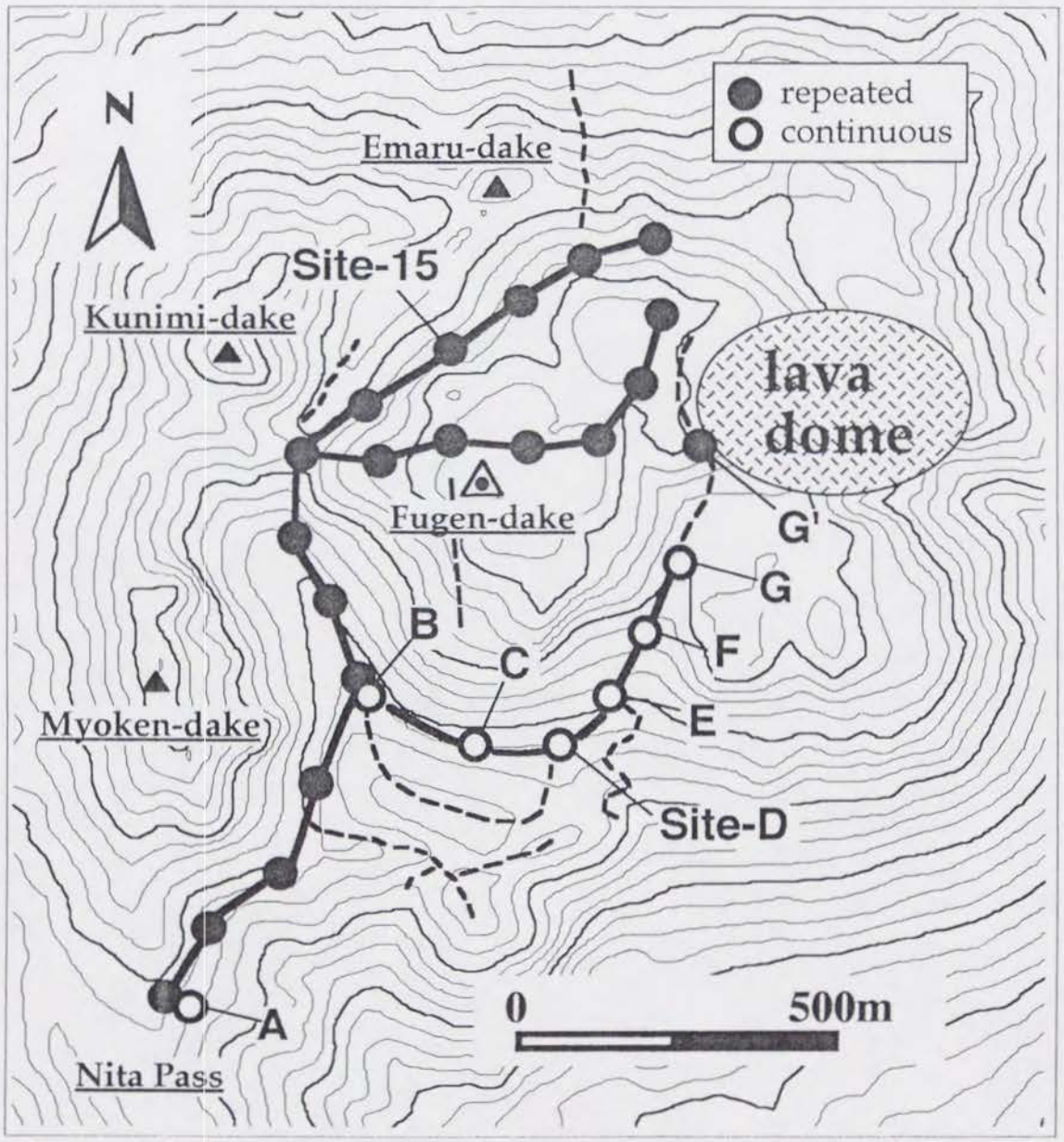
N
repeated
continuous
Emaru-dake
Site-15
Kunimi-dake
lava
dome
Fugen-dake
G'
G
F
B
C
E
Myoken-dake
Site-D
A
0
500m
Nita Pass

Figure 3.1

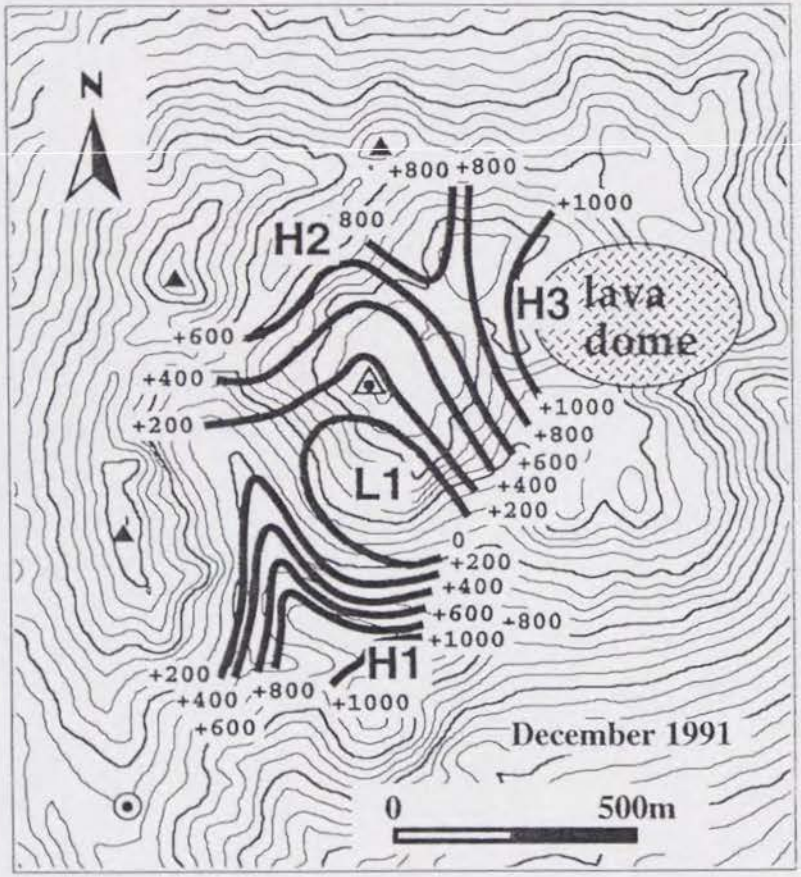

Figure 4.1-(a)

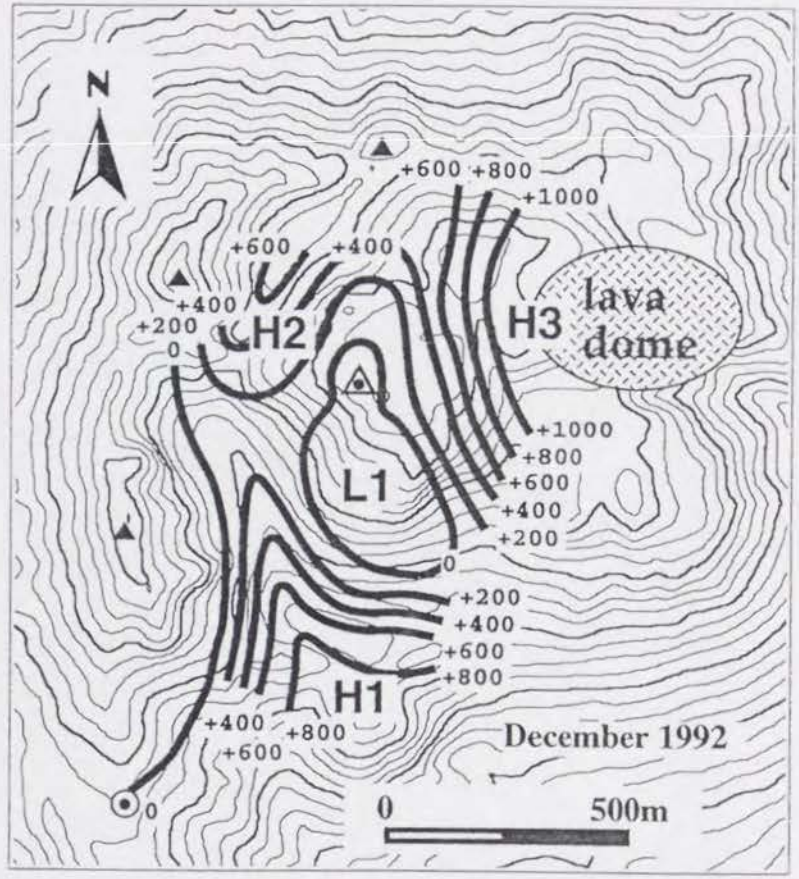

Figure 4.1-(b)

Figure 4.1-(a), (b)

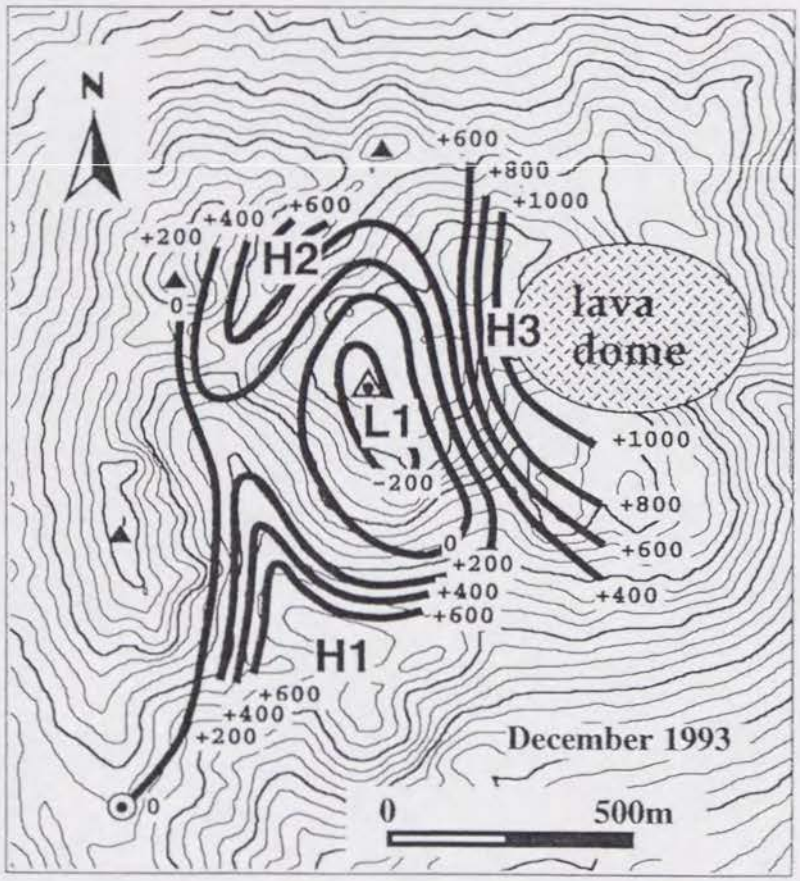

Figure 4.1-(c)

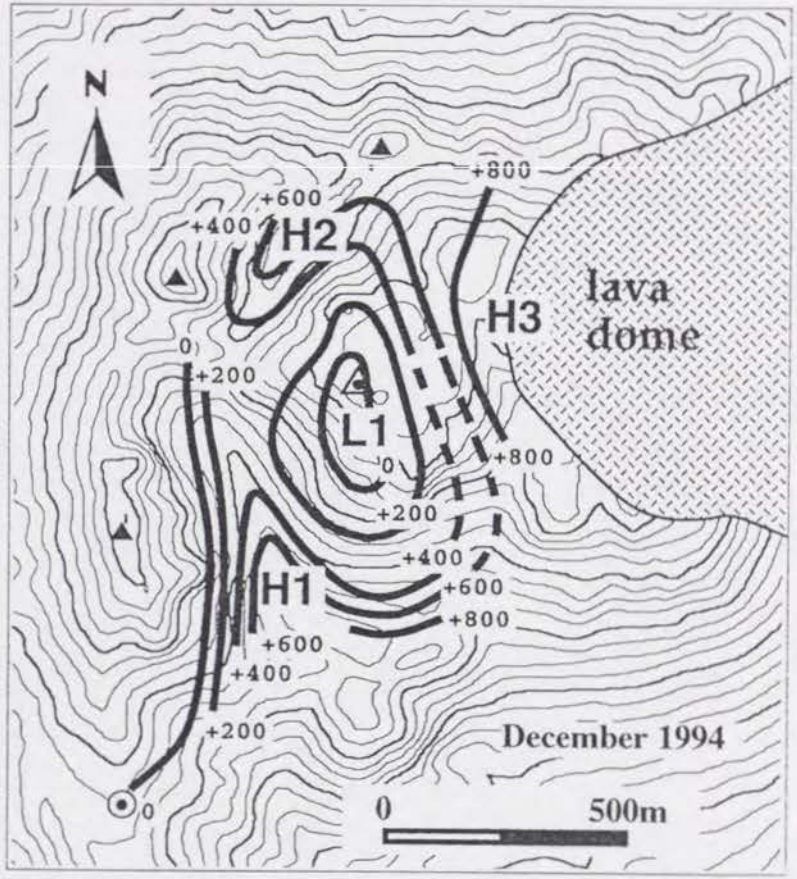

Figure 4.1-(d)

Figure 4.1-(c), (d)

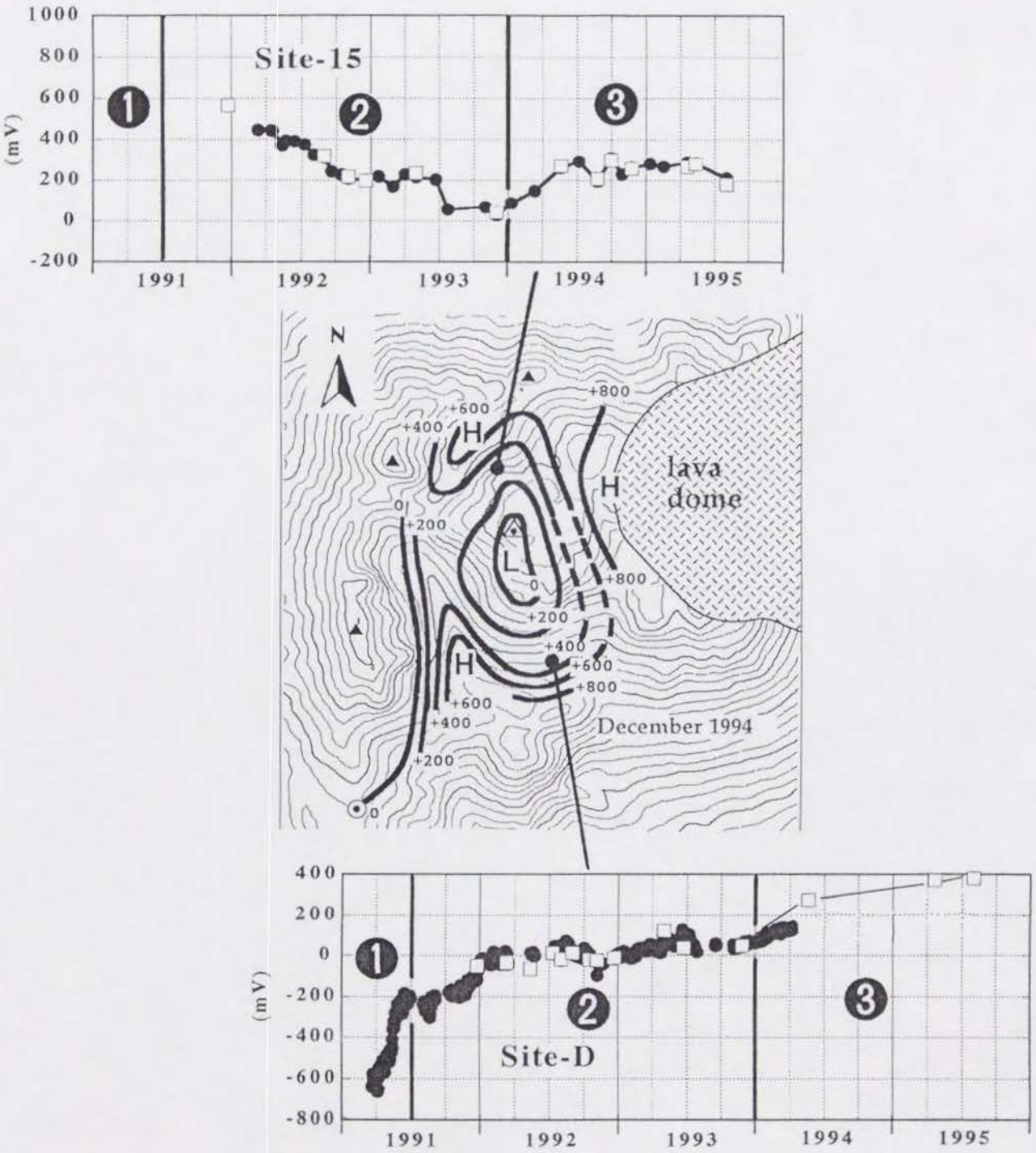
1000
800
600
400
200
0
-200
(mV)
Site-15
1
2
3
1991
1992
1993
1994
1995
N
+800
+600
+400
H
lava
dome
0
+200
L
+800
+200
+400
H
+600
+800
+600
+400
December 1994
+200
0
400
200
0
-200
-400
-600
-800
(mV)
1
2
3
Site-D
1991
1992
1993
1994
1995

Figure 4.2

Figure 5.1-(a), (b)

(a) First Stage (Mar.1991-Jun.1991)
hydrothermal upwelling with magma ascent

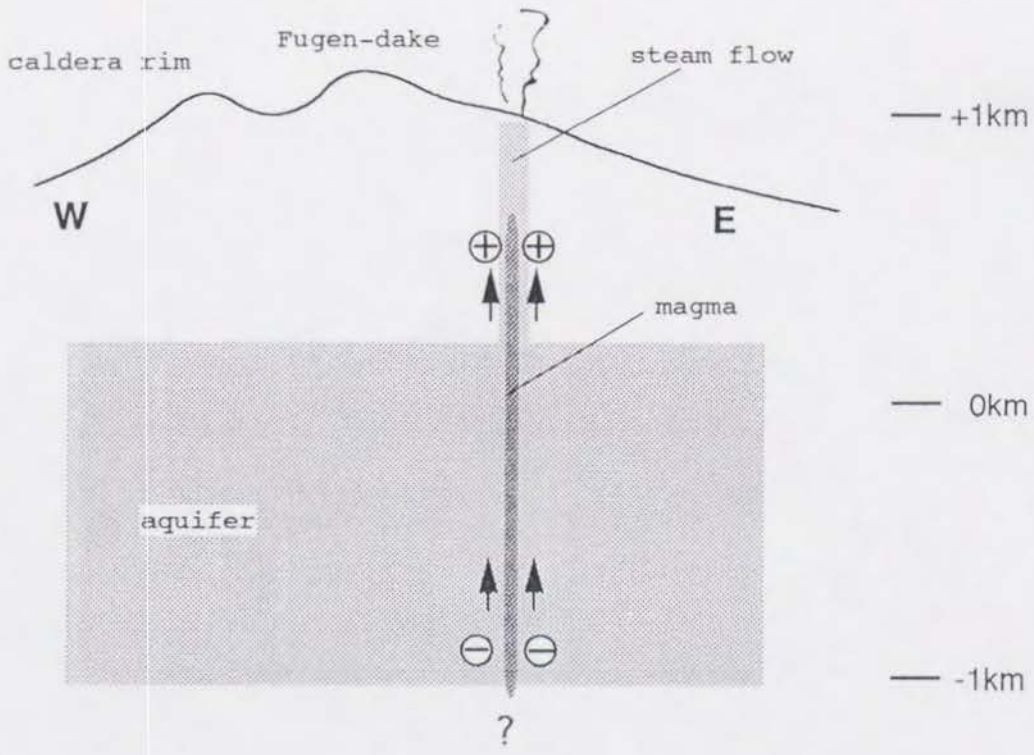

(b) Second Stage (Jun.1991-Dec.1993)
establishment of hydrothermal convection

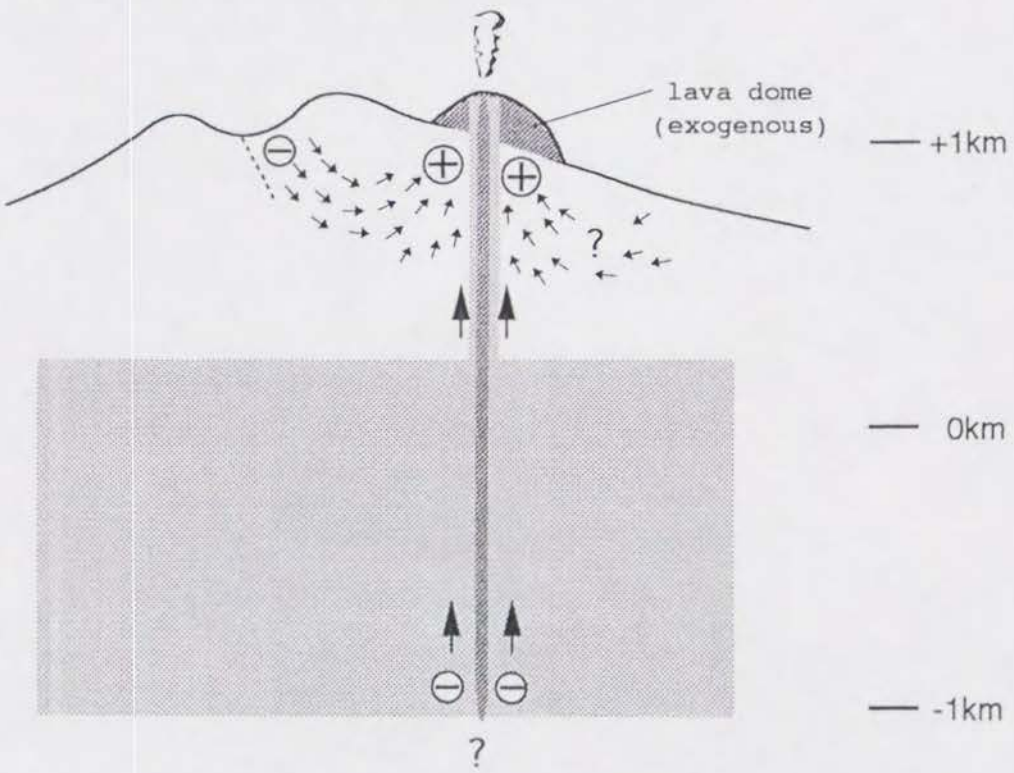

(c) Third Stage (Dec.1993-)
lateral expansion of upwelling area

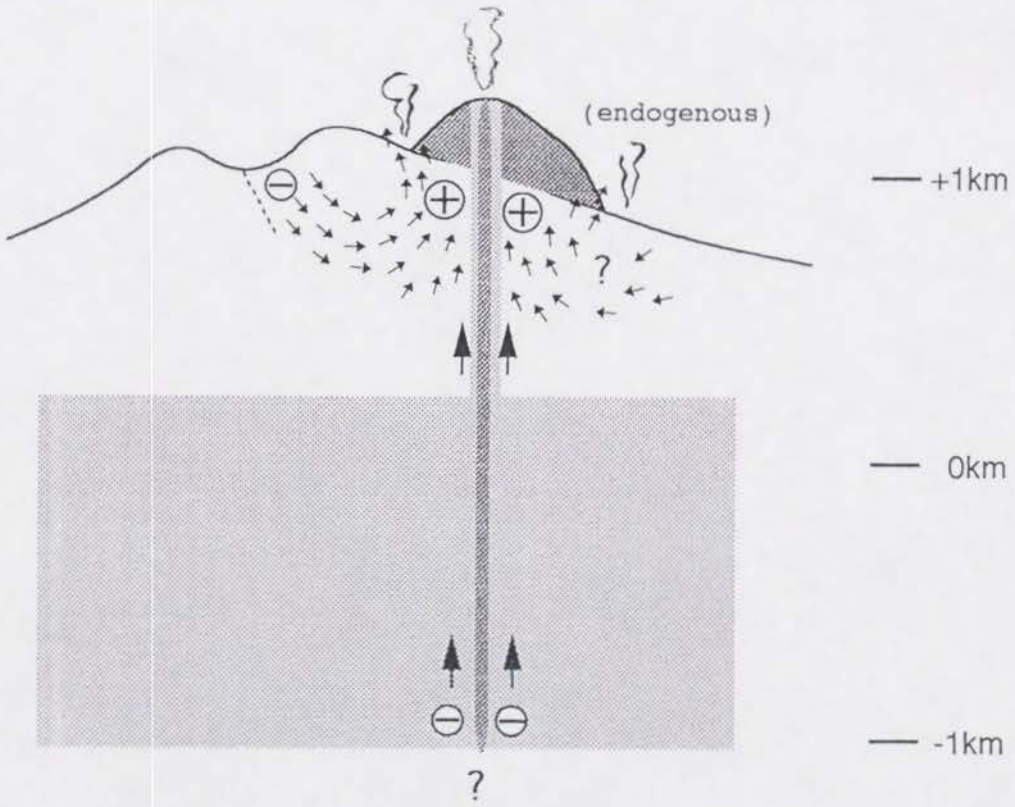

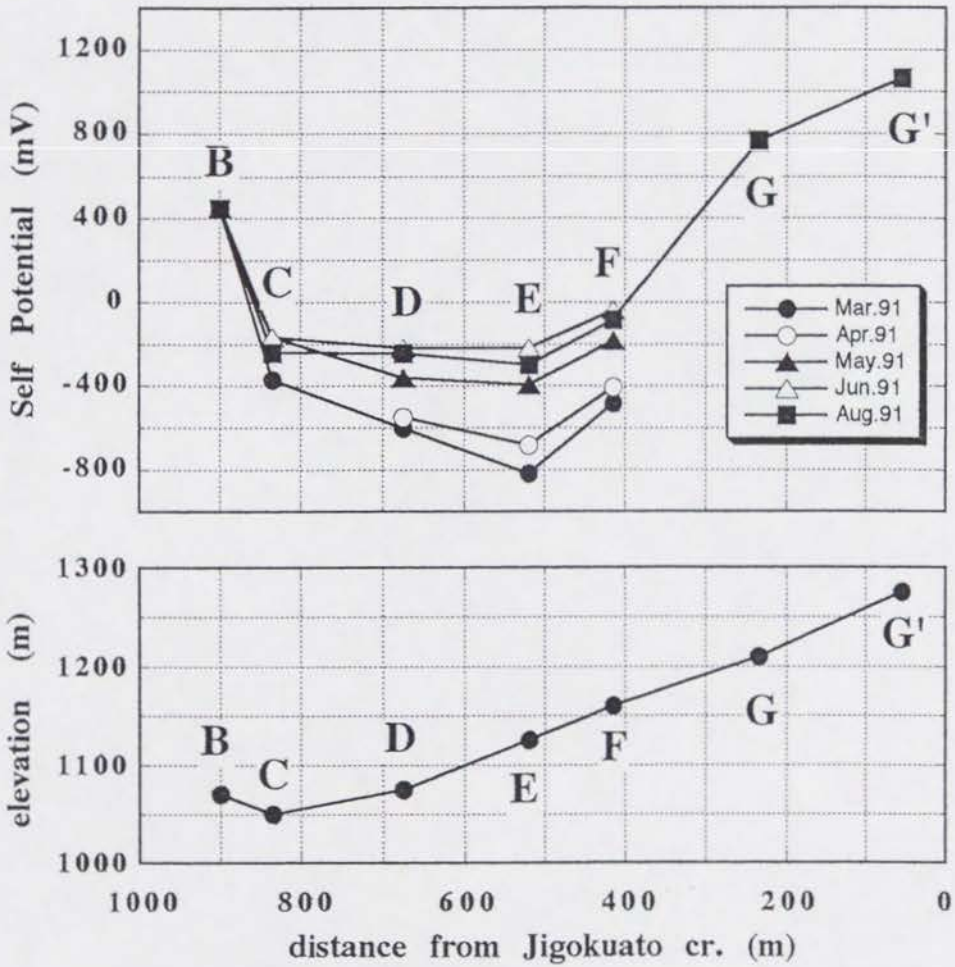

Figure 5.2

Figure 5.2

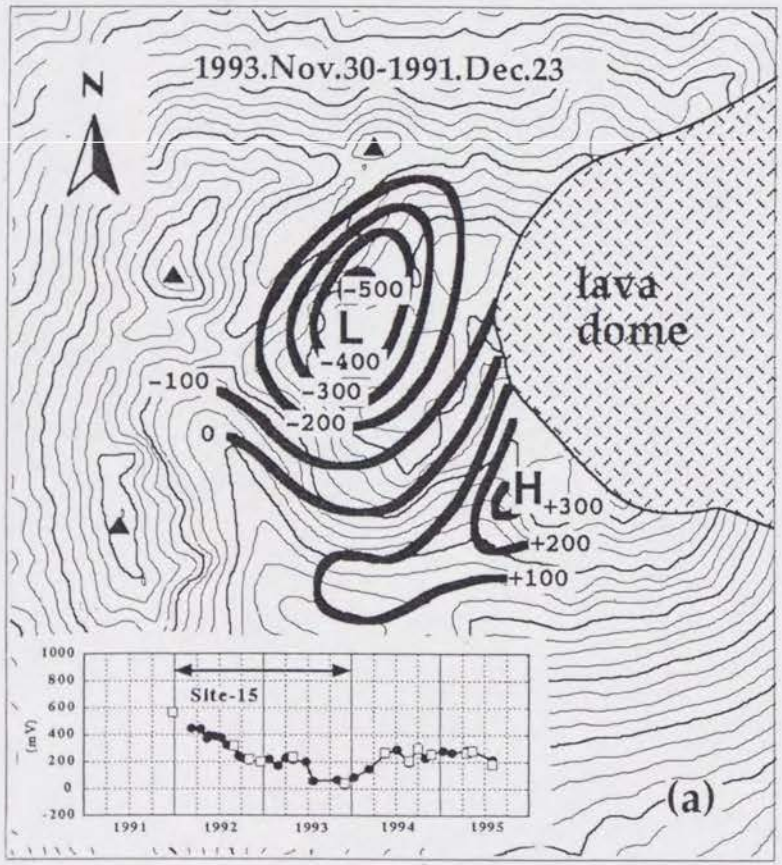

Figure 5.3-(a)

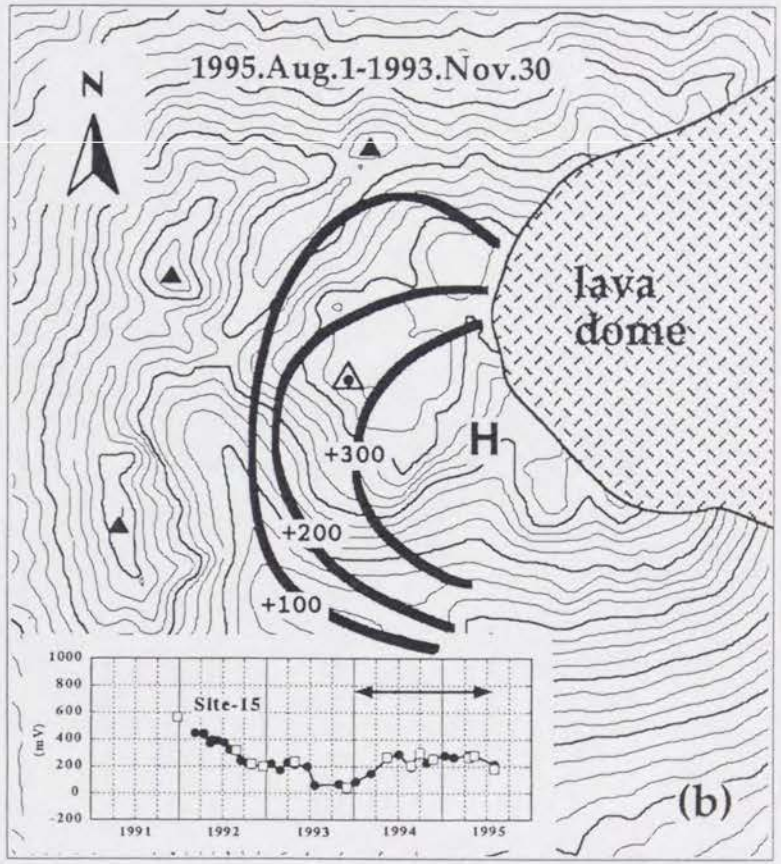

Figure 5.3-(b)

Figure 5.3-(a), (b)

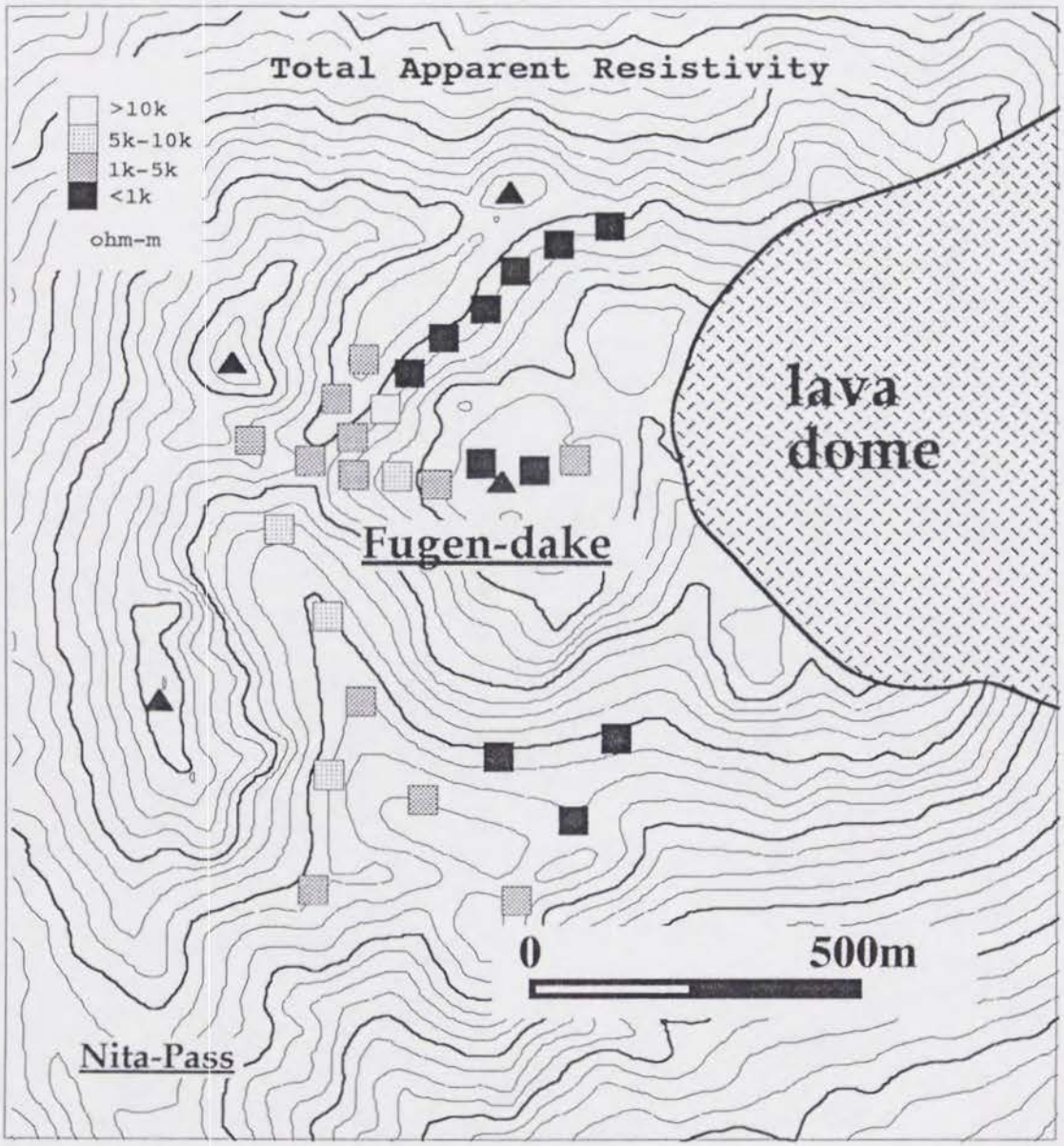
Total Apparent Resistivity
>10k
5k-10k
1k-5k
<1k
ohm-m
lava
dome
Fugen-dake
0
500m
Nita-Pass

Figure 6.1

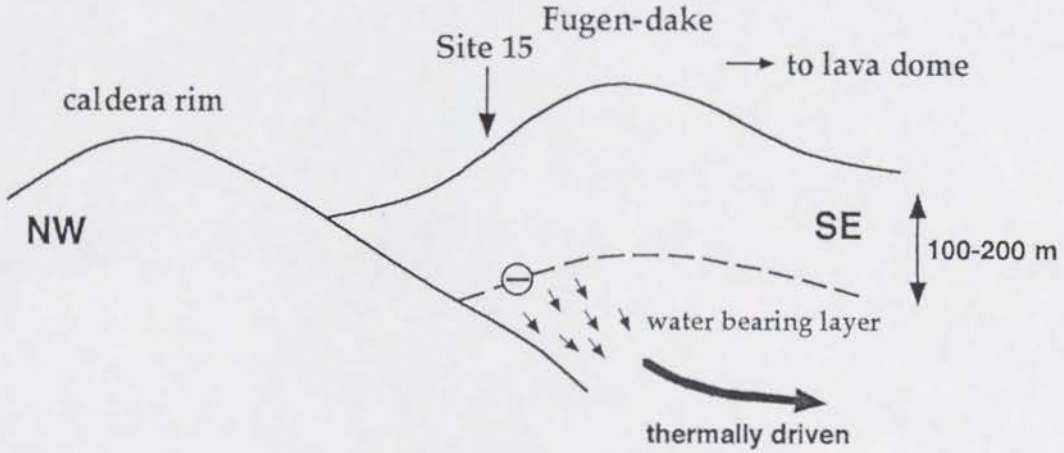

Figure 6.2

Figure 6.2

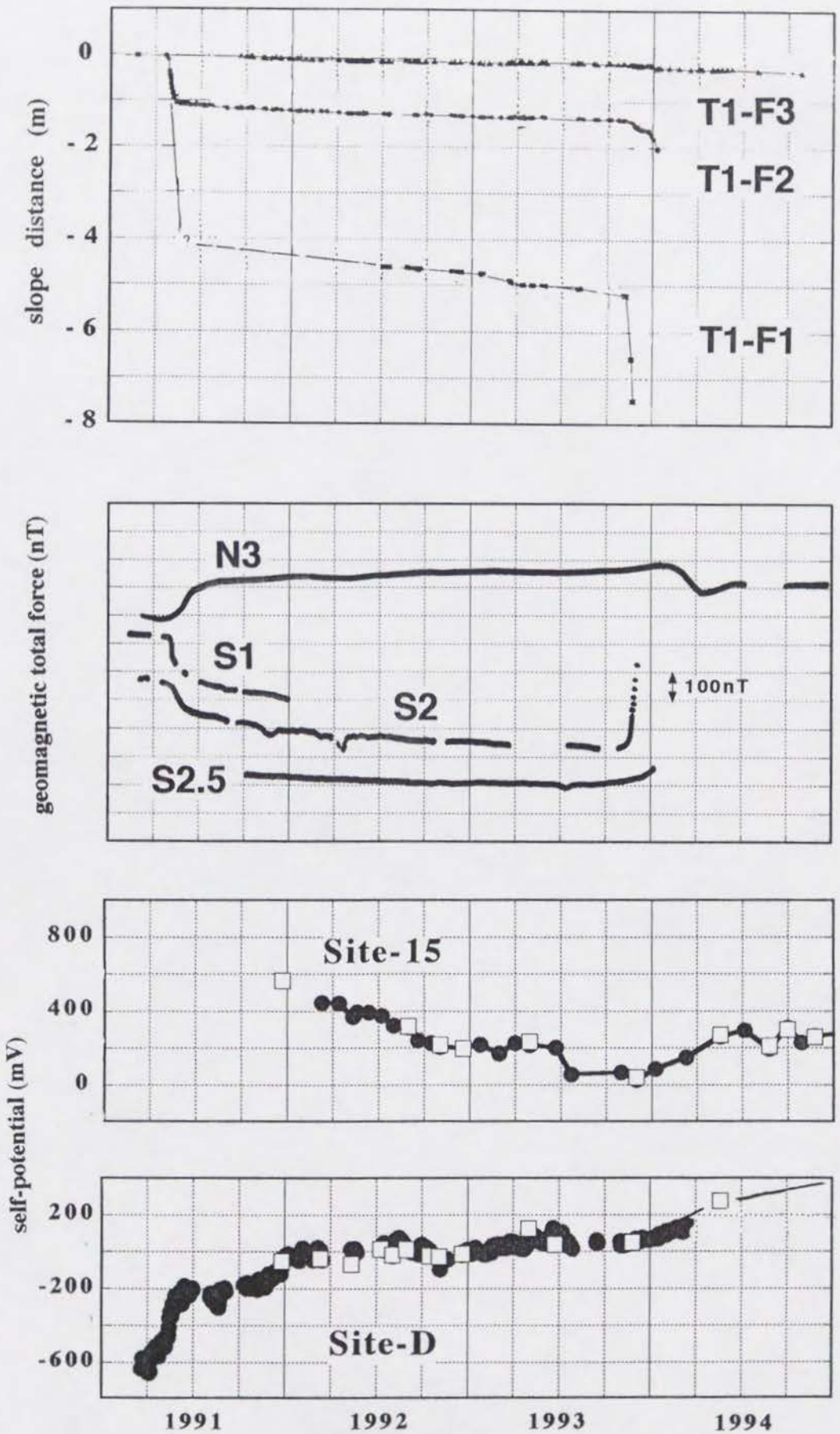
slope distance (m)
0
- 2
- 4
- 6
- 8
T1-F3
T1-F2
T1-F1
geomagnetic total force (nT)
N3
S1
S2
S2.5
100nT
self-potential (mV)
800
400
0
Site-15
200
-200
-600
Site-D
1991
1992
1993
1994

Figure 6.3